

AMES-HET-00-09

BNL-HET-00/31

## Improved Methods for Observing CP Violation in $B^\pm \rightarrow KD$ and Measuring the CKM Phase $\gamma$

David Atwood<sup>a</sup>, Isard Dunietz<sup>b</sup> and Amarjit Soni<sup>c</sup>

*a)* Dept. of Physics, Iowa State University, Ames, IA 50011

*b)* Fermilab, Batavia IL 60500

*c)* Theory Group, Brookhaven National Laboratory, Upton, NY 11973

### Abstract:

Various methods are discussed for obtaining the CKM angle  $\gamma$  through the interference of the charged  $B$ -meson decay channels  $B^- \rightarrow K^- D^0$  and  $B^- \rightarrow K^- \bar{D}^0$  where the  $D^0$  and  $\bar{D}^0$  decay to common final states. It is found that choosing final states which are not CP eigenstates can lead to large direct CP violation which can give significant bounds on  $\gamma$  without any theoretical assumptions. If two or more modes are studied,  $\gamma$  may be extracted with a precision on the order of  $\pm 15^\circ$  given  $\sim 10^8$   $B$ -mesons. We also discuss the case of three body decays of the  $D$  where additional information may be obtained from the distribution of the  $D$  decay products and consider the impact of  $D\bar{D}$  oscillations.

# 1 Introduction

The only manifestations of CP violation observed to the present time are those in the neutral kaon system. The advent of several machines capable of producing large number of  $B$  mesons makes it likely that at least some examples of CP violation in  $B$  physics will soon be seen.

$B$  factories at SLAC and KEK have been specifically constructed to observe CP violation in the time dependent oscillation of  $B^0\overline{B}^0$  when  $B^0$  decays to a CP eigenstate such as  $\psi K_s$  or  $2\pi$ . In such experiments one has the advantage that the CP violating phase may be in a few cases cleanly extracted. In contrast direct CP violation which can occur in  $B^\pm$  decay always appears in combination with a strong phase which cannot be easily determined since it has its origin in strong interaction physics. In order to put the extraction of the CP odd phase on the same footing as the clean oscillation experiments it is thus important that some way of eliminating the uncertainties due to the strong phase be found.

Direct CP violation in  $B^\pm$  decay may prove to be an important component of the future  $B$  physics program because it offers signals sensitive to the angle  $\gamma$  of the unitarity triangle [1]. Here we focus on effects which originate from the interference of  $B^- \rightarrow K^- D^0$  with  $B^- \rightarrow K^- \overline{D}^0$ . In contrast, experiments involving  $B^0$  may only extract  $\alpha$  (from  $B^0 \rightarrow 2\pi$  for instance) and  $\beta$  (from  $B^0 \rightarrow \psi K_S$ ). The unitarity triangle which follows from the unitarity of the CKM matrix is a key prediction of the Standard model. Independent measurements to over determine the triangle by measuring each of its sides and angles therefore provide a non-trivial test of the standard model. Furthermore, the Standard Model predicts that a number of different measurements of CP violation will depend on the same phase  $\gamma$  (e.g. direct CP violation in  $B \rightarrow K\pi$  and oscillations in  $B_s$ ). Comparing the results of these experiments will thus be a sensitive test for new physics.

Since the modes we consider are direct and not time dependent, they may be observed in any experimental setting where large numbers of  $B$  mesons are produced. Aside from the SLAC and KEK asymmetric  $B$ -factories, these include CLEO and hadronic  $B$  experiments such as BTeV, CDF, D0 and LHCb or a high luminosity  $Z$  factory.

A method for putting the determination of  $\gamma$  on the same footing as the oscillation experiments by using direct CP violation was first suggested in [2]

where the decay  $B^- \rightarrow K^- D^0$  is considered followed by the decay of  $D^0$  to a CP eigenstate (see also [3]). In this case the fact that the final state is a CP eigenstate means that it will interfere with the channel  $B^- \rightarrow K^- \bar{D}^0$ . In Section 2, for self containment, we will review the important features of this method and discuss some problems which arise in its implementation.

These problems can be resolved through a more general method using non-CP eigenstates suggested in [4, 5] and refined in [6] which not only enable a clean extraction of  $\gamma$  but in addition have the attractive feature that they can give rise to large CP asymmetries. This is outlined and expanded upon in Section 3 and 4. In Section 5 we estimate some relevant branching ratios and obtain a rough estimate of the attainable accuracy in extracting  $\gamma$ .

In Section 6 we discuss the somewhat more general case where the distributions of three body decays of  $D^0$  are considered. Here we consider two different methods for obtaining  $\gamma$ . First, one can fit the distributions to a resonant channel model where each of the channels can be considered a quasi two body mode. The phases between the channels will thus give additional constraints on the fit. Second, if each point on the Dalitz plot is considered a separate mode, in some cases the accumulated inequality bounds on  $\sin^2 \gamma$  can provide a determination of  $\sin^2 \gamma$ . In section 7 we give our summary and conclusions.

Throughout this paper we will assume that the effects of  $D\bar{D}$  mixing are negligible. In an appendix, we discuss the impact of  $D\bar{D}$  mixing on this method for determining  $\gamma$ . Specifically, if one uses the time interval between the parent  $B^-$  decay and the subsequent  $D$  decay, one can eliminate the effects of mixing. One can also obtain information about  $\gamma$  in time independent studies.

## 2 Using CP Eigenstates Decays of $D^0$

Gronau London and Wyler's strategy (GLW) to extract  $\gamma$  from CP violation in the decay  $B^- \rightarrow K^- D^0$  followed by  $D^0 \rightarrow$  CP eigenstate is to separately determine the branching ratios [2]:

$$(a) \text{ } Br(B^- \rightarrow K^- D^0)$$

$$(b) \text{ } Br(B^- \rightarrow K^- \bar{D}^0)$$

(c)  $Br(B^- \rightarrow K^- D_+^0)$  or  $Br(B^- \rightarrow K^- D_-^0)$

together with their conjugates where  $D_\pm^0$  denote the CP eigenstate  $D_\pm^0 = (D_0 \pm \bar{D}_0)/\sqrt{2}$ .

Once  $a$ ,  $b$ ,  $c$  and the corresponding quantities for the conjugate modes are known then one can separate out the interference effects and thus determine  $\cos(\zeta_K + \gamma)$  and  $\cos(\zeta_K - \gamma)$  simultaneously where  $\zeta_K$  is the CP conserving strong phase difference between  $B^- \rightarrow K^- D^0$  and  $B^- \rightarrow K^- \bar{D}^0$  while  $\gamma$  is the CP violating weak phase difference. From these two cosines, the values of the actual phase angles  $\zeta_K$  and  $\gamma$  can clearly be determined, up to a eight-fold discrete ambiguity as will be discussed in more detail in section 4.

The rate for (c) is experimentally observed through the decay to a CP eigenstate such as  $K^+ K^-$ ,  $K_s \phi$  and  $\pi^+ \pi^-$  and presents no problem in principle. Likewise the decay (a) should be readily measurable through either leptonic or hadronic modes of the  $D^0$ . As it stands, however, this method has a very serious problem in measuring the branching ratio of (b),  $Br(B^- \rightarrow K^- \bar{D}^0)$ . The detector must distinguish  $\bar{D}^0$  from  $D^0$  to determine the decay rate to this rare mode. The background decay  $Br(B^- \rightarrow K^- D^0)$  (i.e. (a)) is expected to be larger by about two orders of magnitude.

There are only two ways that could possibly be used to tag the flavor of the  $\bar{D}^0$ :

(a) through semi-leptonic decays

(b) through hadronic decays

We will consider each of these individually and show that neither is fully satisfactory.

The semi-leptonic tag, i.e. the quark level process  $\bar{c} \rightarrow \ell^- \bar{s} \bar{\nu}_\ell$ , has the problem that there is an overwhelming background from the direct semileptonic decay of the  $B$  meson. The signal here is the sequential decay:

$$B^- \rightarrow K^- \bar{D}^0 \quad ; \quad \bar{D}^0 \rightarrow \ell^- \bar{\nu}_\ell X_{\bar{s}} \quad (1)$$

while the background is from the direct semi-leptonic decay of the  $b$  quark followed by hadronic decays of the charm quark:

$$B^- \rightarrow \ell^- \bar{\nu}_\ell X_c \quad ; \quad c \rightarrow s u \bar{d} \quad (2)$$

Both give rise to the same sign lepton and while there are several features distinguishing the signal from the background it represents a serious problem as the branching ratio for the signal is expected to be  $\mathcal{O}(10^{-6})$  whereas that for the background is expected to be  $\mathcal{O}(10^{-1})$ . The signal/background ratio is thus dauntingly small.

Let us note some of the characteristics of the signal which distinguish it from the background. First of all, in the  $B^-$  rest frame the  $K^-$  tends to be monochromatic. Also the signal tends to yield a pair of kaons  $K^-K^+$  (or  $K^-K^0$ ) whereas the background dominantly has one kaon,  $K^-$  or  $\bar{K}^0$ . In the signal the semi-leptonic decays of the  $\bar{D}^0$  originate from a tertiary vertex in sharp contrast to the case of the background. It is difficult to say whether these distinctions are enough to separate the signal. Detector specific studies are required to give reliable answers but the size of the signal/background ratio does not give us much ground for optimism.

While the use of such a leptonic tag is likely to be impractical, the hadronic decay has a more fundamental problem. In this case one would detect the decay  $B^- \rightarrow K^- \bar{D}^0$  by observing a final state where the  $\bar{D}^0$  decays through a Cabibbo-allowed (CBA) process, for instance  $\bar{D}^0 \rightarrow K^+\pi^-$ . Unfortunately, the doubly-Cabibbo suppressed (DCS) decay of  $D^0$  (e.g.  $D^0 \rightarrow K^+\pi^-$ ) will also lead to the same final state at a branching ratio two orders of magnitude smaller.

On the other hand, as was pointed out in [6], the initial decay  $B^- \rightarrow K^- \bar{D}^0$  is color-suppressed (CLS) while the decay  $B^- \rightarrow K^- D^0$  is color-allowed (CLA). Thus difference in the production rate tends to offset the difference in the decay rates for the two processes and since the final states are really indistinguishable, they will interfere quantum mechanically.

As a specific example consider the possible tag  $\bar{D}^0 \rightarrow K^+\pi^-$ . The signal from  $B^- \rightarrow \bar{D}^0 K^-$  and the background from  $B^- \rightarrow D^0 K^-$  will be given by the sequences:

$$A) B^- \rightarrow K^- \bar{D}^0 \quad ; \quad \bar{D}^0 \rightarrow K^+\pi^- \quad (3)$$

$$B) B^- \rightarrow K^- D^0 \quad ; \quad D^0 \rightarrow K^+\pi^- \quad (4)$$

These two decay chains have the qualitative form.

$$A: \quad CLS \otimes CBA \quad (5)$$

$$B : \quad CLA \otimes DCS \quad (6)$$

Numerically the ratio of these two amplitudes is appreciably close to 1 since it is expected to be given by:

$$\left| \frac{M(B^- \rightarrow K^- D^0 [\rightarrow K^+ \pi^-])}{M(B^- \rightarrow K^- \bar{D}^0 [\rightarrow K^+ \pi^-])} \right|^2 \approx \left| \frac{V_{cb} V_{us}^*}{V_{ub} V_{cs}^*} \right|^2 \left| \frac{a_1}{a_2} \right|^2 \frac{B(D^0 \rightarrow K^+ \pi^-)}{B(\bar{D}^0 \rightarrow K^+ \pi^-)} \quad (7)$$

Here  $a_1$  and  $a_2$  control the relative sizes of the CLA and the CLS amplitudes. Experimentally [7] the indications are that

$$\left| \frac{a_2}{a_1} \right| \approx 0.26 \pm 0.07 \pm 0.05 \quad (8)$$

which roughly agrees with the simple color counting value of  $1/3$ .

Let us consider  $B(D^0 \rightarrow K^+ \pi^-)/B(\bar{D}^0 \rightarrow K^+ \pi^-)$  which is of order  $\lambda^4$ . We can formulate an estimate taking into account SU(3) breaking effects in the form factors and the decay constants. For the present purpose we use the experimental result [8]:

$$\frac{Br(D^0 \rightarrow K^+ \pi^-)}{Br(\bar{D}^0 \rightarrow K^+ \pi^-)} = .0072 \pm .0025 \quad (9)$$

as well as the ratio of CKM elements [8]:

$$\left| \frac{V_{ub}}{V_{cb}} \right| = .08 \pm .02. \quad (10)$$

Then with  $\lambda = 0.23$  and the central values from (Eqns. 8–10) we therefore get:

$$\left| \frac{M(B^- \rightarrow K^- D^0 [\rightarrow K^+ \pi^-])}{M(B^- \rightarrow K^- \bar{D}^0 [\rightarrow K^+ \pi^-])} \right|^2 \approx 1 \quad (11)$$

The two amplitudes are roughly comparable and we cannot tell whether the charmed particle was a  $D^0$  or a  $\bar{D}^0$ .  $B^- \rightarrow K^- \bar{D}^0$  with a  $\bar{D}^0$  decaying hadronically will give rise to a final state which is indistinguishable from the corresponding decay of the  $D^0$  in  $B^- \rightarrow K^- D^0$ . The two amplitudes will thus be subject to large quantum mechanical interference effects. The use

of a hadronic tag for determining  $B(B^- \rightarrow K^- \overline{D}^0)$  for the GLW method appears therefore to be ruled out.

Despite these difficulties, one need not discard the GLW approach. The only input which is lacking is the branching ratio  $B^- \rightarrow K^- \overline{D}^0$ . It may be possible to theoretically estimate this quantity which will allow the GLW program to go forward.

Here we consider an alternative approach where we take advantage of these interference effects to enhance CP violation and ultimately provide another way for a clean (i.e. no penguin pollution) way of extracting  $\gamma$ . As discussed in [6] the fact that these two amplitudes have large interference effects implies that there will be large CP violating asymmetries in such combined decay channels which in turn gives us a handle on measuring  $\gamma$ . Thus, it is instructive to consider why CP violation will be enhanced in this case as compared to GLW.

In the eigenstate case, the size of the expected CP asymmetry is controlled only by the ratio of the amplitudes for  $B^- \rightarrow K^- D^0$  versus  $B^- \rightarrow K^- \overline{D}^0$ . Following the above estimate and taking into account the appropriate CKM factors:

$$\left| \frac{M(B^- \rightarrow K^- \overline{D}^0)}{M(B^- \rightarrow K^- D^0)} \right| \sim \left| \frac{a_2}{a_1} \right| \cdot \left| \frac{V_{ub}}{V_{cb}V_{us}^*} \right| \simeq 0.1 \quad (12)$$

This means that the maximum possible size of the CP asymmetry is expected to be 0(10%). In contrast eq. (11) implies that the two interfering amplitudes have roughly the same magnitude and so the interference effects, and in particular CP violation, will be near maximal.

Of course the search for large direct CP violating signals is interesting in its own right but the real goal is to extract the angle  $\gamma$  from experimental results cleanly, that is without any reference to a model for hadronization. While the original idea of [2], though sound in principle is probably not practical, the basic concept may be used if one observes two or more distinct hadronic states that are common decay products of  $D^0$  and  $\overline{D}^0$  (as all hadronic final states of  $D^0$  are). With this information, one can reconstruct  $\gamma$  cleanly. We now consider a number of methods based on this idea.

### 3 Non-CP Eigenstates Decays of $D^0$

Using this idea, let us now consider the case where the two channels

$$B^- \rightarrow K^- D^0 \quad B^- \rightarrow K^- \overline{D}^0 \quad (13)$$

interfere because both  $D^0$  and  $\overline{D}^0$  decay to some common final state  $X$ . In the GLW method the specific case where  $X$  is a CP eigenstate such as  $K_s \pi^0$  was chosen while we will focus on the instance, considered in [6], where  $X$  is not a CP eigenstate. In particular, following the logic of the previous section, the case where  $D^0 \rightarrow X$  is a DCS decay and  $\overline{D}^0 \rightarrow X$  is a CBA decay is of particular interest, for instance  $X = K^+ \pi^-$ .

In order to formulate an expression for the rates, let us define the following branching ratios:

$$\begin{aligned} a(k) &= Br(B^- \rightarrow k^- D^0) & \overline{a}(k) &= Br(B^+ \rightarrow k^+ \overline{D}^0) \\ b(k) &= Br(B^- \rightarrow k^- \overline{D}^0) & \overline{b}(k) &= Br(B^+ \rightarrow k^+ D^0) \\ c(X) &= Br(D^0 \rightarrow X) & \overline{c}(X) &= Br(\overline{D}^0 \rightarrow X) \\ c(\overline{X}) &= Br(D^0 \rightarrow \overline{X}) & \overline{c}(\overline{X}) &= Br(\overline{D}^0 \rightarrow \overline{X}) \\ d(k, X) &= Br(B^- \rightarrow k^- [X]) & \overline{d}(k, \overline{X}) &= Br(B^+ \rightarrow k^+ [\overline{X}]) \end{aligned} \quad (14)$$

Here  $k^\pm$  represents either  $K^\pm$  or  $K^{*\pm}$  (or indeed one may consider any other kaonic resonance or system of strangeness=-1 and well defined CP) and  $[X]$  is the common  $D^0$  and  $\overline{D}^0$  decay channel observed. Thus the combined rates  $d(k, X)$  and  $\overline{d}(k, \overline{X})$  include the effects of the interference of the two channels.

In the standard model, it is expected that  $a(k) = \overline{a}(k)$ ,  $b(k) = \overline{b}(k)$  and  $\overline{c}(X) = c(\overline{X})$  all of which we will assume from here on. In general, however if  $\gamma \neq 0$  one expects  $d(k, X) \neq \overline{d}(k, \overline{X})$  (CP violation) and indeed the value of the quantities  $d, \overline{d}$  may be expressed in terms of  $a, b$  and  $c$  as:

$$d(k, X) = a(k)c(X) + b(k)c(\overline{X})$$



$$\begin{aligned}
& +2\sqrt{a(k)b(k)c(X)c(\overline{X})}\cos(\zeta_k + \delta_X + \gamma) \\
\overline{d}(k, \overline{X}) = & a(k)c(X) + b(k)c(\overline{X}) \\
& +2\sqrt{a(k)b(k)c(X)c(\overline{X})}\cos(\zeta_k + \delta_X - \gamma)
\end{aligned} \tag{15}$$

where  $\zeta_k$  is the strong phase difference between  $B^- \rightarrow k^- D^0$  and  $B^- \rightarrow k^- \overline{D}^0$ ;  $\delta_X$  is the strong phase difference between  $D \rightarrow X$  and  $D \rightarrow \overline{X}$  and  $\gamma$  is the CP violating weak phase difference between  $B^- \rightarrow k^- D^0$  and  $B^- \rightarrow k^- \overline{D}^0$ .

In the standard model  $\gamma$  is given directly from the CKM elements

$$\gamma = \arg(-V_{ud}V_{ub}^*V_{cb}V_{cd}^*). \tag{16}$$

Existing data does not constrain  $\gamma$  very much giving an allowed range in the SM at 95% c.l. [9] of  $36^\circ \leq \gamma \leq 97^\circ$  corresponding to  $0.35 \leq \sin^2 \gamma$ .

The strong phases  $\zeta_k$  and  $\delta_X$  that result from hadronic final state interactions cannot be reliably calculated with any known method and must be determined experimentally. Here we will take the approach that information about  $\delta_X$  and  $\zeta_k$  are extracted from the data along with  $b(k)$  and  $\gamma$ .

The above may be made somewhat more general by considering the class of modes  $B^- \rightarrow k^- \mathbf{D}$  where  $\mathbf{D}$  is an excited  $D$  meson. Let us suppose that  $\mathbf{D}$  subsequently decays  $\mathbf{D} \rightarrow D + N^0$  where  $N^0$  is a single particle and the  $D$  then decays into a CP non-eigenstate mode of the type we have considered above. For instance  $\mathbf{D}$  may be a  $D^{*0}$  with  $k^- = K^-$  and we may use either of the following decay chains:

$$\begin{aligned}
B^- & \rightarrow K^-(D^* \rightarrow \pi^0[D \rightarrow X]) \\
B^- & \rightarrow K^-(D^* \rightarrow \gamma[D \rightarrow X])
\end{aligned} \tag{17}$$

Here  $D^0 \rightarrow X$  is a DCS mode. In these sort of examples the analysis would be essentially the same as considered for the ground state of the  $D$ . The only constraint on this generalization is that one of  $\{k, \mathbf{D}\}$  should have spin 0 so that there is only one partial wave otherwise multiple partial waves would have to be separated and the analysis for the extraction of  $\gamma$  would be more complicated and has been considered in [10].

## 4 Methods for Extraction of $\gamma$

Let us now turn our attention to the extraction of the weak phase  $\gamma$  and incidentally also the total strong phase  $\xi(k, X) = \zeta_k + \delta_X$ . We will consider two scenarios under which such a reconstruction is possible assuming that the values of  $c(X)$  and  $c(\overline{X})$  have been determined in advance and that the rate of  $D^0\overline{D}^0$  mixing is negligible. In the appendix we show how the possible effects of mixing may be removed from the data.

*Case 1: For one particular mode,  $(k, X)$ ,  $d(k, X)$  and  $\overline{d}(k, \overline{X})$  are known and in addition  $a(k)$  and  $b(k)$  are known.*

This is the simple generalization of the GLW method to the case where  $X$  is not a CP eigenstate. We thus assume that the branching ratio  $b(k)$  may be obtained from tagging the  $\overline{D}$  with the semileptonic decays as discussed in section 2 or as the result of some theoretical estimate [11]. If  $b(k)$  can be obtained in some way, this method is less involved than the other method we will discuss below.

As in the GLW method we are required to extract the interference terms in  $d$  and  $\overline{d}$  by solving the two equations (15) which we can rewrite:

$$\begin{aligned} d(k, X) &= [a(k)c(X) + b(k)c(\overline{X})] [1 + R(k, X) \cos(\zeta_k + \delta_X + \gamma)] \\ \overline{d}(k, \overline{X}) &= [a(k)c(X) + b(k)c(\overline{X})] [1 + R(k, X) \cos(\zeta_k + \delta_X - \gamma)]. \end{aligned} \quad (18)$$

where  $R(k, X)$  is

$$R(k, X) = \frac{2\sqrt{a(k)b(k)c(X)c(\overline{X})}}{a(k)c(X) + b(k)c(\overline{X})} \quad (19)$$

Defining

$$\begin{aligned} \lambda_1 &= \frac{1}{R(k, X)} \left[ \frac{d(k, X)}{a(k)c(X) + b(k)c(\overline{X})} - 1 \right] \\ \lambda_2 &= \frac{1}{R(k, X)} \left[ \frac{\overline{d}(k, X)}{a(k)c(X) + b(k)c(\overline{X})} - 1 \right], \end{aligned} \quad (20)$$

the solution for  $\gamma$  and  $\xi(k, X) = \zeta_k + \delta_X$  is:

$$\begin{aligned}\gamma &= \frac{1}{2}(\sigma \cos^{-1} \lambda_1 - \tau \cos^{-1} \lambda_2) + n\pi; \\ \xi(k, X) &= \frac{1}{2}(\sigma \cos^{-1} \lambda_1 + \tau \cos^{-1} \lambda_2) + n\pi.\end{aligned}\tag{21}$$

In the above  $\sigma, \tau \in \{\pm 1\}$  and  $n \in \{0, 1\}$  expressing the fact that there is a eight fold ambiguity [12] since the sign in front of each of the  $\cos^{-1}$  functions is undetermined and we can add  $\pi$  simultaneously to  $\xi$  and  $\gamma$  without changing the results. Specifically, the eight solutions giving results identical to a given  $(\xi, \gamma)$  are  $\{(\xi, \gamma), (-\xi, -\gamma), (\gamma, \xi), (-\gamma, -\xi), (\pi + \xi, \pi + \gamma), (\pi - \xi, \pi - \gamma), (\pi + \gamma, \pi + \xi), (\pi - \gamma, \pi - \xi)\}$ . To resolve the ambiguities between the strong phase and the weak phase we can use this method on two or more modes since  $\gamma$  will be the same for each mode while  $\xi(k, X)$  should be different. This is a simple generalization of the GLW method discussed in section 2; in that case,  $c(X) = \bar{c}(X)$  while  $\delta_X = n\pi$ .

More generally, if we do consider two decay modes with different strong phases (mod  $\pi$ ), we can dispense with the need to know the value of  $b(k)$  as follows:

*Case 2: For two distinct modes  $\{(k, X_1), (k, X_2)\}$  the quantities  $d(k, X_i)$  and  $\bar{d}(k, \bar{X}_i)$  are known. In addition  $a(k)$  is known but not  $b(k)$ .*

In this case we assume that one cannot easily obtain the branching fraction  $b(k)$  using the semileptonic tag or by any other means. However, if  $d$  and  $\bar{d}$  are known for two different modes, we can solve for the missing information ( $\gamma$  and  $b(k)$  and  $\xi$ ) up to a discrete set of ambiguities.

Specifically, for  $D^0$  decay modes  $X_1$  and  $X_2$  we assume that we have measured the quantities  $\{a(k), c(X_1), c(X_2), c(\bar{X}_1), c(\bar{X}_2)\}$  as well as  $d(k, X_i)$  and  $\bar{d}(k, \bar{X}_i)$ . There are therefore four unknowns that must be solved for:  $\{b(k), \xi_1, \xi_2, \gamma\}$ . To do this we use the four equations:

$$\begin{aligned}d(K, X_1) &= a(K)c(X_1) + b(K)c(\bar{X}_1) + 2\sqrt{a(K)b(K)c(X_1)c(\bar{X}_1)} \cos(\xi_1 + \gamma) \\ \bar{d}(K, \bar{X}_1) &= a(K)c(X_1) + b(K)c(\bar{X}_1) + 2\sqrt{a(K)b(K)c(X_1)c(\bar{X}_1)} \cos(\xi_1 - \gamma)\end{aligned}$$

$$\begin{aligned}
d(K, X_2) &= a(K)c(X_2) + b(K)c(\overline{X}_2) + 2\sqrt{a(K)b(K)c(X_2)c(\overline{X}_2)} \cos(\xi_2 + \gamma) \\
\overline{d}(K, \overline{X}_2) &= a(K)c(X_2) + b(K)c(\overline{X}_2) + 2\sqrt{a(K)b(K)c(X_2)c(\overline{X}_2)} \cos(\xi_2 - \gamma)
\end{aligned}
\tag{22}$$

To solve these, let us define the quantities.

$$\begin{aligned}
u_i &= \frac{b(k)c(\overline{X}_i)}{a(k)c(X_i)}; & y_i &= \frac{d(k, X_i) - \overline{d}(k, \overline{X}_i)}{2a(k)c(X_i)}; & z_i &= \frac{d(k, X_i) + \overline{d}(k, \overline{X}_i)}{2a(k)c(X_i)} - 1; \\
\rho &= \frac{c(X_1)c(\overline{X}_2)}{c(\overline{X}_1)c(X_2)} = \frac{u_2}{u_1}; & \delta &= z_1^2 - z_2^2/\rho - 2(z_1 - z_2)u_1 + (1 - \rho)u_1^2; \\
\epsilon &= y_1^2 - y_2^2/\rho; & Q &= \sin^2 \gamma;
\end{aligned}
\tag{24}$$

where  $y_i$ ,  $z_i$ ,  $\epsilon$  and  $\rho$  are known directly from experiment and  $u_i$  and  $Q = \sin^2 \gamma$  must be solved for.

The equation which  $u_1$  must satisfy is easily derived:

$$4u_1\delta\epsilon = (\epsilon - \delta)(y_1^2\delta - (z_1 - u_1)^2\epsilon) \tag{25}$$

Since  $\delta$  is second order in  $u_1$  this equation is in general a quartic equation which may have up to 4 real roots. For each real root  $(u_1)_k$  (where  $k = 1, \dots, 4$  indexes the solutions of eqn. (25)),  $\sin^2 \gamma$  is given by:

$$\sin^2 \gamma \equiv Q = \frac{\epsilon}{\epsilon - \delta} \tag{26}$$

where  $\delta$  is given in terms of  $u_1$  by Eq. (24). Each root leads to a four fold ambiguity in the determination of  $\gamma$ ; taking up to four roots together there is therefore  $\leq 16$  fold ambiguity in the determination of  $\gamma$ . To reduce this ambiguity (especially if it should turn out that all 16 possibilities manifest), it is therefore helpful if observations are made of at least 3 modes of  $D^0$  decay (for a given  $k$ ) in which case only an overall four fold ambiguity in  $\gamma$  remains. Since this method determines  $Q \equiv \sin^2 \gamma$  it, therefore, cannot distinguish between the solutions  $\{\pm\gamma, \pi \pm \gamma\}$ .

For each solution the corresponding total strong phase difference  $\xi_i$  is then determined without further ambiguity by:

$$\begin{aligned}\sin \xi_i &= \frac{-y_i}{2\sqrt{u_i} \sin \gamma} \\ \cos \xi_i &= \frac{z_i - u_i}{2\sqrt{u_i} \cos \gamma}\end{aligned}\tag{27}$$

Another way to resolve the discrete ambiguity is to determine independently the phase difference:

$$\Delta\xi = \xi_2 - \xi_1 = \delta_{X_2} - \delta_{X_1}\tag{28}$$

from the study of  $D^0$  decays [6, 13]. It is related to the value of  $\gamma$  and  $u_1$  through equation (27) and in general only two values of  $\gamma$  and  $u_1$  will give the correct value of  $\Delta\xi$ , the remaining two fold ambiguity being between  $\gamma$  and  $\gamma + \pi$ .

To qualitatively understand the solutions of these equations, it is useful to consider a plot of  $\gamma$  versus  $b(k)$ . First, let us assume that we have perfect experimental information. For a given decay mode  $X_i$  where we know  $\{a(k), c(X_i), c(\overline{X}_i), d(k, X_i), \overline{d}(k, \overline{X}_i)\}$  while  $\{\xi_i, \gamma, b(k)\}$  remain unknown. The two equations (22) for the mode  $X_i$  give a locus of points in the  $\gamma - b(k)$ , or equivalently the  $\gamma - u_i$  plane when  $\xi_i$  is eliminated. Let us now consider the properties of this curve.

Inspection of these equations shows that they are left unchanged under the transformations:

$$\begin{aligned}(\gamma, \xi_i) &\rightarrow (\pi - \gamma, \pi - \xi) \\ (\gamma, \xi_i) &\rightarrow (-\gamma, -\xi) \\ (\gamma, \xi_i) &\rightarrow (\pi + \gamma, \pi + \xi)\end{aligned}\tag{29}$$

Thus it follows that the curve is periodic with respect to  $\gamma \rightarrow \gamma + \pi$  and that the curve is also symmetric with respect to  $\gamma \rightarrow \pi - \gamma$ . The curve in the range  $0 \leq \gamma \leq \pi/2$  can therefore be reflected through  $\gamma = 0$  and  $\gamma = \pi/2$  to get the entire curve.

For  $\gamma = n\pi$ , the two cosines in eq. (23) are the same so if there is any CP violation the equations are inconsistent. This is obvious from the physics

since  $\gamma$  is the only CP violating parameter; thus  $\gamma = n\pi$  implies there is no CP violation. Conversely, if a finite amount of CP violation is observed, some bound can be placed on  $\gamma$ . In particular, a lower bound  $Q_{min}$  can be placed on  $Q$ :

$$Q > Q_{min} = \frac{1}{2}(1 + z_i)(1 - \sqrt{1 - \alpha'(k, X_i)^2}) \quad (30)$$

and  $\alpha'(k, X_i)$  is the CP asymmetry defined by:

$$\alpha'(k, X_i) = \frac{d(k, X_i) - \bar{d}(k, \bar{X}_i)}{d(k, X_i) + \bar{d}(k, \bar{X}_i)} = \frac{y_i}{1 + z_i}. \quad (31)$$

We also define  $\gamma_{min}$  to be the angle in the first quadrant such that  $Q_{min} = \sin^2 \gamma_{min}$ . Since  $\gamma_{min}$  represents the extreme left edge of the figure eight curve, there is a unique value of  $u_i$  which gives  $Q = Q_{min}$  we will denote this by  $\hat{u}_i$  which is given by:

$$\hat{u}_i = z_i + 2(1 - Q_{min}) \quad (32)$$

Likewise, there can be no CP violation if  $u \rightarrow 0$  or  $u \rightarrow \infty$  and so the observation of CP violation implies an upper and lower bound on the value of  $u$  and hence  $b$ :

$$\begin{aligned} u_{max} &= (1 + \sqrt{z_i - |y_i| + 1})^2 \\ u_{min} &= (1 - \sqrt{z_i + |y_i| + 1})^2 \end{aligned} \quad (33)$$

which leads to the bounds  $b_{min} \leq b(k) \leq b_{max}$  where  $b_{min} = a(k)c(X)u_{min}/c(\bar{X})$  and  $b_{max} = a(k)c(X)u_{max}/c(\bar{X})$ .

Eliminating  $\xi_i$  from the two equations (22) gives a quadratic equation for  $u_i$  for a given value of  $\gamma$  which defines the set of solutions in the  $\gamma - u_i$  plane:

$$Qu_i^2 - 2(z_i + 2(1 - Q))Qu_i + (Qz_i^2 + (1 - Q)y_i^2) = 0. \quad (34)$$

This is quadratic in  $u_i$ ; therefore, there are zero, one or two solutions for  $u_i$  at any given value of  $\gamma$ . In particular, if  $Q < Q_{min}$  there are no solutions while for  $Q = Q_{min}$  there must be exactly one solution (i.e.  $u = \hat{u}$ ). It is also the case that when  $Q = 1$ , for instance, when  $\gamma = \pi/2$ , there is again exactly one solution  $u_i = z_i$ . This follows from the fact that in the sum  $d + \bar{d}$  the interference term vanishes and a value of  $u_i$  may thus be obtained. Taking the  $\gamma$  axis horizontal, the curve in the range  $0 \leq \gamma \leq \pi$  therefore has the topology of a lazy eight centered about the vertical line  $\gamma = \pi/2$  which crosses itself at  $(\pi/2, z_i)$ .

In Fig. 1 we show a plot of  $u_i$  versus  $\gamma$  for  $z_i = 1.5$  and  $y_i = 0, 1, 2$ . The bounds given by Eqns. (30,33) are indicated with the rectangular boxes. Clearly the greater the value of  $y_i$  (and the greater the amount of CP violation), the greater the bounds which may be placed on  $u_i$  and  $\gamma$  through these inequalities by considering just one mode. Thus single modes which have a high degree of CP violation are quite desirable since they lead to the most restrictive bounds in the  $\gamma - u_i$  plot. Indeed, as we have argued above, larger CP violation is more likely to arise in the case of non-CP eigenstate final states (such as  $\bar{D} \rightarrow K^+\pi^-$ ) as compared to CP-eigenstate modes.

Let us now turn our attention to the case when we have two modes present. If we had perfect data concerning each mode, we would generate two of these lazy-eight curves in the  $\gamma - b(k)$  plane. In general, these curves will therefore intersect in as many as four points in the range  $0 \leq \gamma \leq \pi/2$  which correspond to the solution of eq. (25). If the data was inconsistent, then the curves would miss each other corresponding to a situation where eq. (25) has no real solutions for  $\gamma$ . In order to understand how this might play out, let us now consider a scenario for the not yet observed branching ratios.

## 5 Attainable Accuracy

### 5.1 Estimates of Branching Ratios

For the purpose of illustrating the ability to extract  $\gamma$  by combining measurement of several modes, we need to make a simple estimate of the branching ratios of DCS decay modes of  $D$  which have not yet been measured. We will proceed by relating these modes to the well measured Cabibbo-

allowed ones and then use factorization to break down  $D \rightarrow M_1 M_2$  to  $\langle M_2 | J_{cd} | D \rangle \langle M_1 | J_{us} | D \rangle$ . The SU(3) breaking of the decay constants is used in keeping track of the piece  $\langle M_1 | J_{us} | 0 \rangle$ . Single-pole dominance allows one to keep track of the SU(3) breaking in  $\langle M_1 | J_{cd} | D \rangle$ . In the final estimated rates, we also factor in the small difference in phase space.

For a concrete example let us consider the DCS mode  $D^0 \rightarrow K^+ \pi^-$  which we relate in this procedure to CBA counterpart  $D^0 \rightarrow K^- \pi^+$ . Using this reasoning the amplitude will be proportional to:

$$A(D^0 \rightarrow K^+ \pi^-) \propto \lambda^2 f_K (m_D^2 - m_\pi^2) \left(1 - \frac{m_K^2}{m_{D^*}^2}\right)^{-1} \quad (35)$$

Thus

$$\left| \frac{A(D^0 \rightarrow K^+ \pi^-)}{A(D^0 \rightarrow \pi^+ K^-)} \right| = \lambda^2 \left( \frac{f_K}{f_\pi} \right) \left( \frac{1 - m_\pi^2/m_D^2}{1 - m_K^2/m_D^2} \right) \left( \frac{1 - m_\pi^2/m_{D^*}^2}{1 - m_K^2/m_{D^*}^2} \right) \quad (36)$$

In this instance there is no phase space correction. Using  $\lambda = 0.22$ ,  $f_K = 160$  MeV,  $f_\pi = 132$  MeV and other masses we thus get,

$$\begin{aligned} \frac{BR(\overline{D}^0 \rightarrow K^+ \pi^-)}{BR(D^0 \rightarrow \pi^+ K^-)} &= 1.88 \lambda^4 \\ &= 5.3 \times 10^{-3} \end{aligned} \quad (37)$$

Therefore  $BR(D^0 \rightarrow \pi^+ K^-) = 3.83 \times 10^{-2}$  [8] gives:

$$BR(D^0 \rightarrow K^+ \pi^-) = (2.0 \pm .7) \times 10^{-4} \quad (38)$$

which should be compared to the measured value [8]

$$BR(D^0 \rightarrow K^+ \pi^-) = (2.8 \pm 0.9) \times 10^{-4} \quad (39)$$

We will normalize our predictions for all the DCS modes to the measured central value.

For the other DCS modes of interest to us we can now use relations amongst DCS modes and their CBA counterpart. Thus, e.g., for  $D^0 \rightarrow K^+ \rho^-$  we should have:



$$\frac{A(D^0 \rightarrow K^+ \rho^-)}{A(D^0 \rightarrow K^+ \pi^-)} \approx \frac{A(D^0 \rightarrow \pi^+ K^{*-})}{A(D^0 \rightarrow \pi^+ K^-)} \quad (40)$$

Similar scaling relations for the other two modes are:

$$\begin{aligned} \frac{A(D^0 \rightarrow K^+ a_1^-)}{A(D^0 \rightarrow K^+ \pi^-)} &\approx \frac{A(D^0 \rightarrow \pi^+ K_1^-(1270))}{A(D^0 \rightarrow \pi^+ K^-)} \\ \frac{A(D^0 \rightarrow K^{*+} \pi^-)}{A(D^0 \rightarrow K^+ \pi^-)} &\approx \frac{A(D^0 \rightarrow \rho^+ K^-)}{A(D^0 \rightarrow \pi^+ K^-)} \end{aligned} \quad (41)$$

The resulting branching ratio for all the DCS modes of interest are given in Table 1.

To complete our sample calculation, we need to estimate the expected magnitudes of  $\{a, b\}$

Starting with  $a(k)$ , we will extrapolate from the observed branching fraction for related  $B$  decays[8]:

$$\begin{aligned} Br(B^- \rightarrow \pi^- D^0) &= (5.3 \pm 0.5) \times 10^{-3} \\ Br(B^- \rightarrow \rho^- D^0) &= (13.4 \pm 1.8) \times 10^{-3}. \end{aligned} \quad (42)$$

Multiplying this by  $\sin^2 \theta_C$  one obtains the estimates for  $a(k)$ :

$$\begin{aligned} a(K) &\approx 2.6 \times 10^{-4} \\ a(K^*) &\approx 6.6 \times 10^{-4} \end{aligned} \quad (43)$$

The estimation of  $b(k)$  is more uncertain since it is a color suppressed process. Thus, to estimate the branching ratio for  $B^- \rightarrow k^- \bar{D}^0$  we use the fact that the quark level diagram for this process is color suppressed with respect to  $B^- \rightarrow k^- D^0$  and take the color suppression to be simply a factor of  $1/N_c$ . Folding in all the appropriate CKM elements an estimate for the branching ratio may be obtained from the previous estimate of  $a(k)$  (taking  $N_c = 3$ ):

$$\frac{b(k)}{a(k)} \approx \left[ \frac{|V_{ub}||V_{cs}|}{N_c |V_{cb}||V_{us}|} \right]^2 \approx .015 \quad (44)$$

and so for the two specific cases:

$$\begin{aligned} b(K) &\approx 4.0 \times 10^{-6} \\ b(K^*) &\approx 10.0 \times 10^{-6} \end{aligned} \tag{45}$$

## 5.2 CP Violation in Single Modes

Let us now perform some sample calculations using the above estimated branching ratios in order to illustrate what precision might be obtained by this method.

First, we will consider what can be learned through the use of data in a single mode. As discussed above, this will not allow one to obtain an exact value of  $\gamma$  but can give a bound on  $\gamma$  if large CP violation is present. We will therefore consider how many  $B$  decays are needed to have a measurable signal of CP violation and what bounds on  $\gamma$  would follow. We will next consider the precision for extracting  $\gamma$  by combining the data from several modes.

To illustrate this let us consider the specific case of CP violation when  $X = K^+\pi^-$ . The observed [8] branching ratios for the  $D$  decays are:

$$\begin{aligned} c(K^+\pi^-) &= (2.9 \pm 1.4) \times 10^{-4} \\ c(K^-\pi^+) &= (3.83 \pm 0.12) \times 10^{-2} \end{aligned} \tag{46}$$

Where the partial partial rate asymmetry is given by:

$$\alpha'(k, X) = \frac{d(k, X) - \bar{d}(k, \bar{X})}{d(k, X) + \bar{d}(k, \bar{X})} \tag{47}$$

which from equation (15) can be written:

$$\alpha'(k, X) = -\frac{R(k, X) \sin(\zeta_k + \delta_X) \sin \gamma}{1 + R(k, X) \cos(\zeta_k + \delta_X) \cos \gamma} \tag{48}$$

Let  $N_B$  be the total number of  $B^\pm$ . In a given mode, let  $E_i$  be the acceptance times efficiency of a detector and let us denote:

$$\tilde{N}_B = E_i N_B \quad (49)$$

Thus if  $\tilde{N}_B^{3\sigma}(k, X)$  is the number of charged  $B^\pm$  required to observe the partial rate asymmetry at a  $3\sigma$  level with an ideal detector, it is related to the actual number,  $N_B^{3\sigma}(k, X)$ , of  $B^\pm$  by  $E_i N_B^{3\sigma}(k, X) = \tilde{N}_B^{3\sigma}(k, X)$ . In terms of the CP asymmetry,  $\tilde{N}_B^{3\sigma}$  is given by:

$$\tilde{N}_B^{3\sigma}(k, X) = \frac{18}{[\alpha'(k, X)]^2 [d(k, X) + \bar{d}(k, \bar{X})]} \quad (50)$$

In order to obtain a large value of  $\alpha'$  it is clearly necessary to have a large value of  $R(k, X)$  since  $|\alpha'| \leq R(k, X)$ . As defined,  $0 \leq R(k, X) \leq 1$  where  $R(k, X)$  is maximized when  $a(k)c(X) \approx b(k)c(\bar{X})$ . It should be clear that this will happen if the two channels have roughly the same amplitude. In particular, using the numbers in the estimates above,  $R(K^-, K^+\pi^-) \approx R(K^{*-}, K^+\pi^-) \approx 0.94$ . On the other hand if we had considered the case where  $D^0$  decays in a CBA mode, then we would have obtained a much smaller value,  $R(K^-, K^-\pi^+) \approx R(K^{*-}, K^-\pi^+) \approx .02$  and so CP violation would be small.

To completely specify  $\alpha'$  and  $\tilde{N}_B^{3\sigma}$ , of course we also need to know  $\cos \xi \cos \gamma$  and  $\sin \xi \sin \gamma$ . Since these are totally unknown, to get a rough idea of the experimental requirements we will take the sample values  $\cos(\xi) \cos \gamma = 0$  and  $\sin(\xi) \sin \gamma = 1/2$ .

In this example we obtain

$$\begin{aligned} \alpha'(K^-, K^+\pi^-) &\approx \alpha'(K^{*-}, K^+\pi^-) \approx 0.47 \\ \tilde{N}_B^{3\sigma}(K^-, K^+\pi^-) &\approx 17.6 \times 10^7 \\ \tilde{N}_B^{3\sigma}(K^{*-}, K^+\pi^-) &\approx 7.0 \times 10^7 \end{aligned} \quad (51)$$

Using the estimated branching ratios in Table 1, we can perform a similar estimate for some of the other possible modes:

$$\tilde{N}_B^{3\sigma}(K^-, K^+\rho^-) \approx 6.3 \times 10^7$$

$$\begin{aligned}
\tilde{N}_B^{3\sigma}(K^{*-}, K^+\rho^-) &\approx 2.5 \times 10^7 \\
\tilde{N}_B^{3\sigma}(K^-, K^+a_1^-) &\approx 9.3 \times 10^7 \\
\tilde{N}_B^{3\sigma}(K^{*-}, K^+a_1^-) &\approx 3.7 \times 10^7 \\
\tilde{N}_B^{3\sigma}(K^-, K^{*+}\pi^-) &\approx 13.6 \times 10^7 \\
\tilde{N}_B^{3\sigma}(K^{*-}, K^{*+}\pi^-) &\approx 5.4 \times 10^7
\end{aligned} \tag{52}$$

where the asymmetries  $\alpha'$  for these modes are given in Table 2.

Since each of these modes as well as several other possibilities have a different values of  $\xi_X$  it is at least likely that a few instances of this kind of CP violation can be observed in the  $\tilde{N}_B^{3\sigma} \sim 10^8$  range.

For comparison let us consider one of the CP eigenstate modes as in GLW, using the above numbers. In this case  $X = X_{CP}$  is a CP eigenstate. In particular, let us take the mode  $X_{CP} = K_S\pi^0$ . Using the  $k = K^*$  case we have as before  $a(K^*) = 6.6 \times 10^{-4}$ ;  $b(K^*) = 10.0 \times 10^{-6}$ . In this case  $c(K_S\pi^0) = \bar{c}(K_S\pi^0) = 1.05 \times 10^{-2}$ . From this we get  $R = 0.24$ . Here  $\delta = 0$  so making a similar assumption as above concerning the phases, that  $\sin\zeta \sin\gamma \approx 1/2$  and  $\cos\zeta \cos\gamma \approx 0$  we obtain  $\alpha'(K^*, K_S\pi^0) \approx 0.12$ . Substituting this into equation (50) we obtain  $\tilde{N}_B^{3\sigma} \approx 9.0 \times 10^7$ .

In principle we can improve this by folding in information from all possible modes that are CP eigenstates<sup>1</sup>. Some particular  $D^0$  decay modes which are CP eigenstates are

$$\begin{aligned}
\{3K_s, K_s\eta, K_s\rho^0, K_s\omega, K_s\eta', K_sf_0, K_s\phi, \\
K_sf_2, \pi^+\pi^-, K^+K^-\}
\end{aligned} \tag{53}$$

Using the observed branching fraction in [8] these have a total branching fraction of about 5% (if the corresponding modes with  $K_L$  are included, this total roughly doubles). Using the effective  $c$  obtained with the CP non-eigenstate method from all of these modes together, we get  $\tilde{N}_B^{3\sigma}(K^{*-}, X_{CP}) \approx 1.9 \times 10^7$  which is roughly what we obtained in the single mode  $\tilde{N}_B^{3\sigma}(K^{*-}, K^+\rho^-) \approx 2.5 \times 10^7$ . Thus, although the event rate for the various DCS modes is smaller than the CP eigenstate modes, the CP violating asymmetries are larger and  $\tilde{N}_B^{3\sigma}$  is comparable. The latter case does have the following potential advantages

---

<sup>1</sup>In particular we add the  $d(k, X)$  for CP even states to  $\bar{d}(k, X)$  for CP odd states and vice versa

1. Each mode has a different strong phase difference and so it is perhaps more likely that one will have a total strong phase near  $\pm\pi/2$  (i.e. maximal CP violation).
2. Since  $\alpha'$  tends to be larger, the bounds placed on  $\gamma$  will tend to be more restrictive.

In order to illustrate these two points, Fig. 2 shows the locus of allowed points on a plot of  $\gamma$  versus  $b(K^*)$  which would be obtained with the example above in the case of a  $K^+\pi^-$  final state (solid line) and a  $K_S\pi^0$  final state (dashed line) assuming an ideal measurement. Clearly, in this instance the restriction on  $b(k)$  and  $\gamma$  is much tighter for the  $K^+\pi^-$  final state than for the  $K_S\pi^0$  final state.

### 5.3 Combining Information From Several Modes

Let us now consider the degree of accuracy in the determination of  $\gamma$  that may be obtained through the combination of various modes. To do this, we will do an illustrative calculation of the 90% confidence levels one can obtain on the  $\gamma - b(k)$  plane with  $\tilde{N}_B^{3\sigma} = 10^8$ .

To produce a scenario, we will consider some specific values of  $\gamma$  and  $\xi_i$  together with the branching ratios above and then calculate the values of  $d$  and  $\bar{d}$  which would be relevant. If we now take these as being the experimental value we can then consider the likelihood as a function of  $\gamma$  and  $b(k)$ .

The modes we will consider are ( $D^0 \rightarrow K^+\pi^-$ ,  $D^0 \rightarrow K_S\pi^0$ ,  $D^0 \rightarrow K^+\rho^-$ ,  $D^0 \rightarrow K^+a_1^-$ ,  $D^0 \rightarrow K^0\rho^0$  and  $D^0 \rightarrow K^{*+}\pi^-$ ). We will take  $\tilde{N}_B = 10^8$  and consider  $k = K^*$ . It is important to note that in this example we consider statistical errors only. It is clear that in order to perform such a study, systematic errors must be under control.

The exact experimental results will, of course depend on the strong phases and  $\gamma$ . For the purposes of illustration, let us assume that  $\gamma = 60^\circ$  and the strong phases:

$$\begin{aligned}
\xi(K^+\pi) &= 10^\circ & \xi(K_S\pi^0) &= 20^\circ \\
\xi(K^+\rho^-) &= 30^\circ & \xi(K^+a_1^-) &= 40^\circ \\
\xi(K_S\rho^0) &= 200^\circ & \xi(K^{*+}\pi^-) &= 50^\circ
\end{aligned} \tag{54}$$

Numerically, the values of  $d$  and  $\bar{d}$  are given in Table 2 where the  $d_i$ ,  $\bar{d}_i$  entries are given in units of  $10^{-8}$ .

In Fig 3a and 3b we show the likelihood contours as a function of  $\gamma$  and  $b(K^*)$ . In Fig 3a we consider only the data from the  $K^+\pi^-$  and  $K_s\pi^0$  final states<sup>2</sup>. The solid curve shows the locus of solutions which explain the  $K^+\pi^-$  data while the dashed curve shows the solutions which explain the  $K_s\pi^0$  data. As can be seen there are four intersections which is the case in general when just two modes are considered. The contour regions correspond to 68% and 90% confidence levels based on  $\tilde{N}_B^{3\sigma} = 10^8$ . In Fig. 3b we consider the situation where data from all six modes is used. In this figure, the solution for  $K^+\pi^-$  is shown in solid,  $K_s\pi^0$  with short dashes,  $K^+\rho^-$  with long dashes,  $K^+a_1^-$  with the dash-dot line,  $K_s\rho^0$  with the dash-dot-dot line and  $K^{*+}\pi^-$  with the dash-dash-dot line. As can be seen from this figure, the correct value of  $\gamma$  and  $b(k)$  is now identified with the only ambiguity being the four fold ambiguity in  $\gamma$  between  $\pm\gamma$  and  $\pi \pm \gamma$ .

In Fig. 4 we have projected the likelihood from Fig. 3b onto the  $\gamma$  axis where we have considered the case of  $\gamma = 15^\circ, 30^\circ, 60^\circ$  and  $90^\circ$  which are indicated by the curves peaked at those values of  $\gamma$ . In each of these cases, the 90% confidence interval is about  $\pm 10^\circ$  about the solution.

It should be realized that three body states  $K^+\rho^-$ ,  $K_s\rho^0$  and  $K^{*+}\pi^-$  can all lead to the common final state  $K_s\pi^+\pi^-$ . If one examines the distribution in phase space, then the vector resonances overlap to some extent and the channels will interfere with each other. In the following section, we will discuss how the additional information implicit in this situation can assist in extracting the value of  $\gamma$ .

## 6 Using Three Body Decays

Here we will consider the generalizations of the two approaches considered in section 4 to the case of a three body decay. First of all, we can consider the three body decay as consisting of a number of quasi two body channels

---

<sup>2</sup>Note that it has been suggested[12] that the combination of a DCS mode and a CP eigenstate mode (as in this example) offers some advantage because of the larger statistics that can be obtained by combining different eigenstate modes. This may be the case although how well a particular combination works also depends to a great degree on the strong phases.

which we can regard as distinct modes and find a solution for  $b(k)$  and  $\gamma$ . A second approach is to regard each point of the Dalitz plot as a distinct mode. We can then apply the inequalities eqns. (30,33) at each point. Since all of these inequalities must be true simultaneously, a very stringent bound can generally be placed on  $\gamma$  and  $b(k)$ . In fact we will argue that for at least some points this inequality is an equality so the limit given by such an argument should in fact give  $\gamma$  and  $b(k)$ .

As an example we will consider in particular the case of  $D^0$ ,  $\bar{D}^0 \rightarrow K^+\pi^-\pi^0$ . In this case the CBA decay  $\bar{D}^0 \rightarrow K^+\pi^-\pi^0$  has been experimentally studied by the E687 collaboration [14]. The data they obtain is fit to an amplitude to a general multi-channel 3-body decay form:

$$\mathcal{M}(\bar{D}^0 \rightarrow K^+\pi^-\pi^0) = a_0 e^{i\delta_0} + \sum_i a_i \exp(i\delta_i) B(a, b, c|r) \quad (55)$$

where  $r$  is a label for the resonance and  $a, b$  and  $c$  are labels for the three final state particles which are permuted so that  $(a, b)$  forms the resonance that a given term represents. Thus, the function  $B$  is given by  $B(a, b, c|r) = BW(a, b|r)\mathcal{S}(a, c)$  where if  $J_r$  is the spin of  $r$ ,

$$\begin{aligned} BW(a, b|r) &= -(s_{ab} - m_r^2 + i\Gamma_r(s_{ab})m_r)^{-1} \\ \mathcal{S}(a, c) &= \begin{cases} 1 & \text{if } J_r = 0 \\ -2\vec{P}_a \cdot \vec{P}_c & \text{if } J_r = 1 \\ 2 \left( 3(\vec{P}_a \cdot \vec{P}_c)^2 - |\vec{P}_a|^2 |\vec{P}_c|^2 \right) & \text{if } J_r = 2 \end{cases} \quad (56) \end{aligned}$$

where  $s_{ab} = (p_a + p_b)^2$  and  $\vec{P}_a$  and  $\vec{P}_c$  are the 3-momenta of  $a$  and  $c$  in the  $ab$  rest frame and

$$\Gamma_r(s_{ab}) = \Gamma_r(m_r^2) \left( \frac{m_r^2 |\vec{P}_a|^2}{(m_r^4 + m_a^4 + m_b^4 - 2m_r^2 m_a^2 - 2m_r^2 m_b^2 - 2m_a^2 m_b^2)} \right)^{J_r + \frac{1}{2}} \quad (57)$$

Here  $m_r$  is the mass of the resonance and  $\Gamma_r$  is the energy dependent width.

Thus, the general model used in [14] for a 3-body decay includes a number of resonance channels, each of which may have a different spin and phase  $\delta_i$  together with a non-resonant term (i.e.  $a_0 \exp(i\delta_0)$ )

Specifically, for  $\overline{D}^0 \rightarrow K^+ \pi^- \pi^0$  they use a non-resonant term together with three channels:

$$\begin{aligned} \overline{\mathcal{M}} = & a_0 \exp(i\delta_0) + a(K^{*0}) \exp(i\delta_{K^{*0}}) B(K^+ \pi^- \pi^0 | K^{*0}) \\ & + a(K^{*+}) \exp(i\delta_{K^{*+}}) B(K^+ \pi^0 \pi^- | K^{*+}) \\ & + a(\rho^-) \exp(i\delta_{\rho^-}) B(\pi^- \pi^0 K^+ | \rho^-) \end{aligned} \quad (58)$$

In this analysis[14] the decay fractions<sup>3</sup> for each channel and the relative phases were determined which we have summarized in Table 3. In our calculation we will use these decay fractions together with the global average for the total branching ratio,  $Br(\overline{D}^0 \rightarrow K^+ \pi^- \pi^0) = 13.9 \pm 0.9\%$  given in [8]. For the purposes of our illustrative calculations we will assume that these quantities take on their central values.

The DCS decay  $D^0 \rightarrow K^+ \pi^- \pi^0$  has not likewise been investigated experimentally, so for the purposes of making numerical estimates, we will use a model based on SU(3). First we write a decomposition of  $\mathcal{M}$  similar to that of eq. (58):

$$\begin{aligned} \mathcal{M}(D^0 \rightarrow K^+ \pi^- \pi^0) = & a'_0 \exp(i\delta'_0) + a'(K^{*0}) \exp(i\delta'_{K^{*0}}) B(K^+ \pi^- \pi^0 | K^{*0}) \\ & + a'(K^{*+}) \exp(i\delta'_{K^{*+}}) B(K^+ \pi^0 \pi^- | K^{*+}) \\ & + a'(\rho^-) \exp(i\delta'_{\rho^-}) B(\pi^- \pi^0 K^+ | \rho^-) \end{aligned} \quad (59)$$

Using the relations between the branching ratios to two body decays discussed in section 5.1, we can relate the magnitudes  $|a'(K^{*0})|$ ,  $|a'(K^{*+})|$  and  $|a'(\rho^-)|$  to  $|a(K^{*0})|$ ,  $|a(\rho^-)|$  and  $|a(K^{*+})|$  by regarding them as amplitudes for quasi-two body decays. In addition we set  $|a'_0| = \lambda^2 |a_0|$ . Assuming exact SU(3) for the phases of the DCS channels, they will be:

---

<sup>3</sup> The decay fraction for a given channel  $X$  is the rate of  $D^0 \rightarrow K^+ \pi^- \pi^0$  if all channels aside from  $X$  are turned off divided by the total rate of  $D^0 \rightarrow K^+ \pi^- \pi^0$  with all channels present. Thus, for instance, the decay fraction through  $K^{*+} \pi^-$  is  $Br(\overline{D}^0 K^{*+} \pi^-) Br(K^{*+} \rightarrow K^+ \pi^0)$ . Due to interference effects, the decay fractions need not add up to 1.



$$\delta'_0 = \delta_0 \quad \delta'_{K^{*0}} = \pi + \delta_{K^{*0}} \quad \delta'_{K^{*+}} = \delta_{\rho^-} \quad \delta'_{\rho^-} = \delta_{K^{*+}} \quad (60)$$

This model then predicts:

$$Br(D^0 \rightarrow K^+ \pi^- \pi^0) = 7.8 \times 10^{-4} \quad (61)$$

The only free parameters now are the strong phase difference  $\xi$  between  $B^- \rightarrow k^- D^0$  and  $B^- \rightarrow k^- \overline{D}^0$ , the overall branching ratios  $a(k)$  and  $b(k)$  and of course  $\gamma$ . If we use the estimates of  $a(K^*)$  and  $b(K^*)$  discussed in section 5, we can therefore obtain the Dalitz plots of the  $K^+ \pi^- \pi^0$  final state which resulting from interference of  $D^0$  and  $\overline{D}^0$  channels.

Fig. 5a shows such a plot with  $\gamma = 90^\circ$  and  $\xi = 70^\circ$  which is intended to represent a sample of  $\tilde{N}_B^{3\sigma} = 10^{10}$ . The upper plot represents  $B^-$  decays where the variables used are  $s = (p_{\pi^-} + p_{K^+})^2$  and  $t = (p_{\pi^0} + p_{\pi^-})^2$  while the lower plot represents the CP conjugate.

It is clear that in this case there is significant amount of CP violation. In Fig. 5b we have taken  $\xi = 160^\circ$  and again it is clear that CP violation is present but here it is more subtle. There are about the same number of points in each of the plots but the distribution changes going from  $B^-$  to  $B^+$ .

In these plots, the three resonant bands are prominent, one could isolate the resonant contributions by fitting the plot to a model such as discussed above and thus obtain four modes (the three resonances plus the non-resonant contributions) to feed into the analysis of the previous section. Obviously there is more information implicit in these distributions. For instance, one would have additional constraints since one would know the relative strong phase difference between each of the  $D$  decay modes.

In particular, for this model one has the magnitudes of four amplitudes each for  $B^-$  and  $B^+$  decay (giving 8 parameters) and three phase differences<sup>4</sup> giving a total of 14 parameters. The three unknowns in this case are just  $\gamma$ ,  $b(k)$  and  $\zeta$  so they are well over-determined.

In order to get an idea of how many B mesons are required to extract useful information from this kind of data, let us consider what is required to

---

<sup>4</sup>one cannot determine an overall phase so only the differences between the  $\delta$ 's can be extracted from measurements

find a 3- $\sigma$  signal of CP violation for this system. In Fig. 6a we show a plot of the overall partial rate asymmetry for this mode for  $\gamma = 90^\circ$  as a function of the overall strong phase difference  $\eta$ . In Fig. 6b we show with the solid line the number of  $B^0$  ( $\tilde{N}_B^{3\sigma}$ ) mesons required to give a statistical 3- $\sigma$  signal for the partial rate asymmetry.

When the partial rate asymmetry is small, for instance in the case where  $\eta = 160$  in Fig. 5b, clearly  $\tilde{N}_B^{3\sigma}$  becomes large but of course, we are not using the information contained in the full distribution. Using the methods of [15] if we assume the CBA and DCS decays of the  $D^0$  are understood we can construct an observable or system of weights of various regions of the Dalitz plot which is optimally sensitive to CP violation. Using this method,  $\tilde{N}_B^{3\sigma}$  is shown in Fig. 6b with the dashed curve; depending on  $\eta$ ,  $\tilde{N}_B^{3\sigma}$  varies between  $(0.35 - 2) \times 10^8$ .

Another approach to obtaining  $\gamma$  is to use the generalization of the bound given in eqn. (30). If one fits the Dalitz plots to continuous curves, then, regarding each point as a separate mode, we would have  $Q_{min} \leq Q$  as a function of the Dalitz plot variables. Since each lower bound must be valid, the maximum lower bound,  $\hat{Q} = \max(Q_{min})$  will provide the most stringent lower bound on  $Q$  so therefore  $Q \geq \hat{Q}$ .

In fact it is not unreasonable to expect that  $\hat{Q} = Q$ . To see this note that eqn. (32) tells us that if  $Q = Q_{min}$ , then

$$u = z_i + 2 \cos^2 \gamma = u + 2\sqrt{u} \cos \gamma \cos \xi + 2 \cos^2 \gamma \quad (62)$$

so therefore

$$\cos \xi = -\cos \gamma / \sqrt{u} \quad (63)$$

If eqn. (63) is true anywhere on the Dalitz plot, then  $\hat{Q} = Q$  and one would expect that this condition would apply on some curve on the dalitz plot. This is illustrated in Fig. 7a where the locus of points where  $Q = Q_{min}$  is shown for  $\gamma = 60^\circ$  with  $\zeta = 0^\circ$  (solid line);  $\zeta = 30^\circ$  (dashed line);  $\zeta = 60^\circ$  (dotted line) and  $\zeta = 90^\circ$  (dot-dashed line).

To extract  $Q$  using this method, it is useful to consider the function

$$f(q) = \frac{\int_{Dalitz} \theta(Q_{min}(s, t) - q) ds dt}{\int_{Dalitz} ds dt} \quad (64)$$

where the integral is over the allowed region of the Dalitz plot and  $\theta(x) = 0$  if  $x < 0$  or 1 if  $x \geq 0$ . Thus  $f(q)$  is the fraction of the Dalitz plot such that  $Q_{min} \geq q$ . For values of  $q \rightarrow Q$  from below,  $f(q) \propto \sqrt{Q - q}$  and so  $f^2(q)$  will linearly extrapolate its endpoint at  $q = Q$ .

In Fig. 7b we show a plot of  $f(rQ)$  where  $r = 0.7$  and  $0.9$  as a function of  $\gamma$  for  $\zeta = 0^\circ$  (solid);  $\zeta = 30^\circ$  (dashed);  $\zeta = 60^\circ$  (dotted) and  $\zeta = 90^\circ$  (dot-dashed). From this is apparent that for almost every combination of strong and weak phases roughly 20% of the dalitz plot has  $Q_{min} \geq 0.9Q$ .

In Fig. 7c we show a graph of  $f^2(q)$  for  $\zeta = 90^\circ$  with  $Q = 0.25$ ,  $Q = 0.5$ ,  $0.75$ . As can be seen, in all cases a significant fraction of the Dalitz plot has  $Q_{min}$  close to  $Q$  and the curves extrapolate linearly to an endpoint at  $q = Q$ .

Likewise we can extract  $b(k)$  by applying eqn. (33) to each point of the Dalitz plot. Here one has both an upper and a lower bound on  $b(k)$  so that if one considers the functions:

$$\begin{aligned} g_{min}(b) &= \frac{\int_{Dalitz} \theta(b_{min}(s, t) - b) ds dt}{\int_{Dalitz} ds dt} \\ g_{max}(b) &= \frac{\int_{Dalitz} \theta(b - b_{min}(s, t)) ds dt}{\int_{Dalitz} ds dt} \end{aligned} \quad (65)$$

the support of  $g_{min}$  must lie entirely below  $b(k)$  while the support of  $g_{max}$  must lie entirely above  $b(k)$ . As with the bound in  $Q$ , the end point of the support in both cases is  $b(k)$ .

In Fig. 8 we show a graph of  $g_{min}^2(b)$  and  $g_{max}^2(b)$  as a function of  $b/b(k)$  in the case of  $D^0 \rightarrow K^+\pi^-\pi^0$ . Here we take  $\gamma = 60^\circ$  and  $\zeta = 90^\circ$ . Again a significant portion of the Dalitz plot can be seen to give values of  $b_{min}$  and  $b_{max}$  close to the endpoint.

If  $b(k)$  were determined in this way, the information could easily be combined with the branching ratio to a two body final state (e.g.  $K^+\pi^-$  or CP eigenstates) to obtain  $\gamma$  as discussed in Case 1 of section 4.

We can also apply the methods discussed in this section to the case where the  $D^0$  decays to a 2-body final state (eg.  $D^0 \rightarrow K^+\pi^-$  or  $K_S\pi^0$ ) but the parent  $B^-$  decays to a 3-body final state, for instance  $B^- \rightarrow D^0 K_S \pi^-$ . In this case, of course the Dalitz plot variables are those of the parent  $B^-$  decay but other than that, one could solve for  $\gamma$  by fitting the the distribution to a series of amplitudes which could be treated as different modes or by finding  $\hat{Q}_{min}$  as described above.

## 7 Summary and Conclusion

In conclusion, we have considered a number of ways of observing the interference between  $B^- \rightarrow K^- D^0$  and  $B^- \rightarrow K^- \overline{D}^0$  as a means of cleanly extracting  $\gamma$ . In general, this is achieved by observing final states common to  $D^0$  and  $\overline{D}^0$  decay. To fully determine  $\gamma$  with such observations, several different decay modes must be observed or else the difficult to measure decay rate for  $B^- \rightarrow K^- \overline{D}^0$  must be independently known.

Thus if for one  $D^0$  decay mode  $X$  the branching ratios for  $B^- \rightarrow K^- X$  and  $B^+ \rightarrow K^+ \overline{X}$  are known, where the  $X$  results from the interference of  $D^0$  and  $\overline{D}^0$  channels and if one also knows  $B^- \rightarrow K^- \overline{D}^0$  then  $\gamma$  can be determined up to an 8 fold ambiguity. The special case where  $X$  is a CP eigenstate was originally considered in [2].

On the other hand if the branching ratio for  $B^- \rightarrow K^- \overline{D}^0$  is not known but there is a large degree of CP violation in the mode, then it may be possible to put a lower bound on  $\sin^2 \gamma$ . A particularly promising class of decays which could give large CP asymmetries are cases where  $D^0 \rightarrow X$  is a DCS decay. In such cases the enhancement of the decay  $\overline{D}^0 \rightarrow X$  which is CBA is balanced by the enhanced production amplitude  $B^- \rightarrow K^- D^0$  which is CLA. The two channels thus have roughly equal amplitudes therefore CP asymmetries can be large.

If two or more modes  $X_1, \dots, X_n$  are measured, then we no longer need to know  $B^- \rightarrow K^- \overline{D}^0$ , it can be fit for along with  $\gamma$ . In the case of 2 modes there is potentially a 16 fold ambiguity due to the need for solving of a quartic equation in  $\sin^2 \gamma$ . If 3 or more modes are considered, then there is only a 4-fold ambiguity since the system of equations for  $\sin^2 \gamma$  is over determined. In our sample calculation it was found that for  $\hat{N}_B = 10^8$ , that the 90% bound on  $\gamma$  found from combining several modes is roughly  $15^\circ$  which is typical although the actual precision depends on the values of the strong phase differences.

This approach can be generalized to the case where the  $D^0$  undergoes a 3-body (or indeed  $n$ -body) decay. If one considers each point in the dalitz plot to be a single mode, one can obtain a lower bound for  $\sin^2 \gamma$  at each point. In general, one expects that the maximum lower bound is in fact equal to  $\sin^2 \gamma$  so this method actually gives  $\gamma$  up to a four fold ambiguity. The same method may also be applied to determine  $b(k)$  by obtaining upper and lower

bounds on  $b(k)$  at each point. Alternatively, fitting the Dalitz distributions to a resonant channel model provides enough information to obtain  $\gamma$ .

Although throughout we have assumed that  $D\bar{D}$  mixing is negligible, in the appendix we show how the effects of such mixing may be eliminated by using information about the time between the  $B^-$  and  $D^0$  decays at the expense of increasing the statistical errors by about  $\sqrt{2}$ .

This research was supported in part by the U.S. DOE contracts DE-FG02-94ER40817 (ISU) and DE-AC-76CH00016 (BNL).

## Appendix: The Implications of $D^0 - \bar{D}^0$ Mixing

In the discussion so far we have explicitly assumed that  $D^0\bar{D}^0$  was negligible. In particular, since we often take advantage of interferences involving DCS decays which are  $O(1\%)$  of the interfering CBA decay, the total probability of mixing must be less than  $O(1\%)$  for the above formulation to remain valid. In this section we consider the generalization to the case where  $D\bar{D}$  mixing may be present.

We will argue that for final states which involve the DCS decay of the  $D^0$  (such as  $B^- \rightarrow K^- [D^0 \rightarrow K^+ \pi^-]$ ) the effects of such mixing will be at most  $O(10\%)$  on the rates (i.e.  $d(k, X)$ ).

In particular there are two possible ways to deal with mixing

1. Using information on the the time between the  $B^-$  decay and the subsequent  $D^0$  decay, then the effects of possible mixing can be eliminated.
2. If the parameters of  $D\bar{D}$  mixing are known independently, then they can be taken into account in interpreting the time integrated data

Indeed, if the mixing parameters and time dependent data is available, then one can in principle extract  $\gamma$  from just one mode though most likely, the time dependence in the decay is too weak to make this a useful method.

In order to examine the question, let us first define the standard parameterization of this mixing as described in [16]. We denote the mass eigenstates as

$$|D_L\rangle = p|D^0\rangle + q|\overline{D}^0\rangle \quad |D_H\rangle = p|D^0\rangle - q|\overline{D}^0\rangle \quad (66)$$

where  $D_L$  and  $D_H$  represent the light and heavy eigenstates respectively. If we denote the ratio

$$q/p = r_{qp}e^{2i\phi} \quad (67)$$

where  $\phi$  is a CP violating phase which could, in principle, be present in  $D^0 - \overline{D}^0$  mixing and CP is also violated if  $r_{qp} \neq 1$  though here we will suppose that  $r_{qp} \approx 1$  as would likely be the case for CP violation generated by physics beyond the SM.

Let us denote by  $m_H$  and  $m_L$  the mass of the  $D_H$  and  $D_L$  states respectively. Likewise, we denote by  $\Gamma_H$  and  $\Gamma_L$  the widths of these states. In terms of these quantities, we will use the definitions:

$$\begin{aligned} m &= \frac{m_H + m_L}{2}, & \Gamma &= \frac{\Gamma_H + \Gamma_L}{2}, & \mu &= m - i\Gamma/2, \\ \Delta m &= m_H - m_L, & \Delta\Gamma &= \Gamma_H - \Gamma_L, \\ x_D &= \frac{\Delta m}{\Gamma}, & y_D &= \frac{\Delta\Gamma}{2\Gamma}, & z_D &= x_D + iy_D \equiv Ze^{i\lambda}, \end{aligned} \quad (68)$$

and denote by  $|D_{phys}(t)\rangle$  and  $|\overline{D}_{phys}(t)\rangle$  the time evolved state which is created at  $t = 0$  as  $D_{phys}^0$  and  $\overline{D}_{phys}^0$  respectively. These are thus related to the flavor eigenstates as:

$$\begin{aligned} |D_{phys}(t)\rangle &= g_+(t)|D^0\rangle + r_{qp}e^{2i\phi}|\overline{D}^0\rangle; \\ |\overline{D}_{phys}(t)\rangle &= g_+(t)|\overline{D}^0\rangle + r_{qp}^{-1}e^{-2i\phi}|D^0\rangle \end{aligned} \quad (69)$$

with  $g_{\pm}$  are given by:

$$g_+(t) = e^{-i\mu t} \cosh\left(\frac{i}{2}z_D\tau\right); \quad g_-(t) = e^{-i\mu t} \sinh\left(\frac{i}{2}z_D\tau\right). \quad (70)$$

with  $\tau = \Gamma_D t$ .

A number of experiments have recently produced results which bound these mixing parameters. The E791 experiment at Fermilab obtains[17]  $\Delta\Gamma = 0.04 \pm 0.14 \text{ ps}^{-1}$  corresponding to  $y = 0.8 \pm 2.9 \pm 1.0\%$  from the study of the life time ratio of  $D^0 \rightarrow K^-\pi^+$  versus  $D^0 \rightarrow K^+K^-$ . CLEO has reported[18] a 95% c.l. bound of  $|x'| \leq 2.8\%$  and  $-5.8\% < y' < 1.0\%$  where  $x' = x \cos \delta_{K^+\pi^-} + y \sin \delta_{K^+\pi^-}$  and  $y' = -y \sin \delta_{K^+\pi^-} + x \cos \delta_{K^+\pi^-}$  obtained through the study of the time dependence of the decay  $D^0 \rightarrow K^+\pi^-$ . Results from the FOCUS experiment[19] at Fermilab, again using the lifetime ratio, give  $y = 3.42 \pm 1.39 \pm 0.74\%$  which interestingly is  $2.5\text{-}\sigma$  from 0.

In the Standard Model,  $D^0 - \bar{D}^0$  mixing receives contributions from both short distance and long distance processes. The short distance mixing via the box diagram may be reliably estimated to be  $y_D < x_D = O(10^{-5})$ . On the other hand, the long distance effects involve considerable uncertainty from the hadronic interactions involved. Calculations based on dispersion theory [20] suggest that  $|z_D| < 10^{-4}$ . On the other hand it has recently been suggested [21] that life time differences driven by kaonic resonances in the vicinity of the  $D^0$  mass could lead to  $y_D \sim 10^{-2}$ . In the Standard Model, the CP violating phase  $\phi$  will in all cases be negligible.

It is also possible that  $D^0 - \bar{D}^0$  mixing is driven by new physics beyond the standard model. Many examples of such mixing have been considered (see compilation in [22]) and in this case, additional CP violation through the phase angle  $\phi$  is also possible.

In the case we are interested in,  $B^- \rightarrow K^-[D^0 \rightarrow X]$ , the initial decay is to a mixed state of  $D^0 - \bar{D}^0$  where both the  $D^0$  and  $\bar{D}^0$  components have some amplitude to decay to  $X$ . Since  $X$  is small, it is justified to expand the mixing effects on the time dependent decay as follows:

$$\begin{aligned} \frac{d}{d\tau}d(k, X) &\approx (d_0(k, X) + d_1(k, X)\tau)e^{-\tau} \\ \frac{d}{d\tau}\bar{d}(k, \bar{X}) &\approx (\bar{d}_0(k, \bar{X}) + \bar{d}_1(k, \bar{X})\tau)e^{-\tau} \end{aligned} \quad (71)$$

Since  $d_0$  and  $\bar{d}_0$  represent the decay rate at 0 time interval, they will be identical with the expressions given in eq. (22). If we assume that there is no CP violation in the  $D\bar{D}$  system, then  $d_1$  and  $\bar{d}_1$  are given by:

$$\begin{aligned}
\frac{1}{2}(d_1 + \bar{d}_1) &= +2\sqrt{ac(\bar{X})}Z \left\{ \sqrt{ac(X)} \sin(\lambda + \delta) \cos \gamma + \sqrt{bc(\bar{X})} \sin(\lambda - \zeta) \cos(\gamma + \phi) \right\} \\
&\quad + 2\sqrt{bc(X)}Z \left\{ \sqrt{bc(\bar{X})} \sin(\lambda - \delta) \cos \gamma + \sqrt{ac(X)} \sin(\lambda + \zeta) \cos(\gamma + \phi) \right\} \\
\frac{1}{2}(d_1 - \bar{d}_1) &= -2\sqrt{ac(\bar{X})}Z \left\{ \sqrt{ac(X)} \cos(\lambda + \delta) \sin \gamma + \sqrt{bc(\bar{X})} \cos(\lambda - \zeta) \sin(\gamma + \phi) \right\} \\
&\quad + 2\sqrt{bc(X)}Z \left\{ \sqrt{bc(\bar{X})} \cos(\lambda - \delta) \sin \gamma + \sqrt{ac(X)} \cos(\lambda + \zeta) \sin(\gamma + \phi) \right\}
\end{aligned} \tag{72}$$

In order to estimate the relative effect of the mixing, let us assume that  $Z \approx 0.01$  and recall from our rough estimates that

$$\frac{b}{a} \approx \frac{c(X)}{c(\bar{X})} \approx 0.01 \tag{73}$$

and thus from eq. (72) we can estimate:

$$\frac{d_1}{d_0} \approx \frac{\bar{d}_1}{\bar{d}_0} \approx 0.1 \tag{74}$$

Note that in Eqn. (72) the time dependent term depends on both  $\zeta$  and  $\delta$  rather than just the sum  $\xi$  and, in addition, it depends on the mixing parameters. The simplest way to extract  $\gamma$  given time dependent data is therefore to try and obtain the values of  $d_0$  and  $\bar{d}_0$  which do not have these extra dependences reducing the problem to the same situation as if mixing were not present.

This can be accomplished through weighting the data with

$$w_0(\tau) = 2 - \tau \tag{75}$$

so that

$$d_0 = \int_0^\infty [d(\tau)w_0(\tau)]d\tau; \quad \bar{d}_0 = \int_0^\infty [\bar{d}(\tau)w_0(\tau)]d\tau \tag{76}$$



Using this method more data would be required to obtain the same statistical results as in the unmixed case. In the unmixed case where  $d_1 = 0$  one could obtain  $d_0$  more effectively by taking the time integrated rate. Thus in the unmixed case if a measurement of  $d_0$  is based on  $n$  events, the uncertainty in  $d_0$  is given by:

$$\frac{(\Delta d_0)^2}{d_0^2} = \frac{1}{n} \quad (\text{no mixing}) \quad (77)$$

In the mixed case, using eqn. (76) the uncertainty is

$$\frac{(\Delta d_0)^2}{d_0^2} = \frac{2}{n} \left(1 + \frac{d_1}{d_0}\right)^2 \quad (\text{with mixing}) \quad (78)$$

From Eqn. (74) this means that roughly twice the data is needed to have the same statistical power as in the unmixed case. In order to gauge the precision of time measurement required, we can smear out the distribution in eq. (76) with a Gaussian resolution function of the form

$$r(\tau, \tau') \propto e^{-\frac{(\tau - \tau')^2}{2\sigma^2}} \quad (79)$$

where  $\tau$  is the actual time of the decay,  $\tau'$  is the measured time of the decay and  $\sigma$  is the resolution (all in units of  $1/\Gamma_D$ ). Since  $r$  is symmetric under  $\tau \leftrightarrow \tau'$ , the fact that  $w$  is linear in  $\tau$  implies eq. (76) will still be true for  $\tau'$  but now the error is:

$$\frac{(\Delta d_0)^2}{d_0^2} = \frac{2}{n} (1 + \sigma^2) \left(1 + \frac{d_1}{d_0}\right)^2 \quad (80)$$

As can be seen, the number of events required is not adversely effected if  $\sigma \leq 1/\Gamma_D$  but will be significantly degraded otherwise.

In the above strategy, it was assumed that the mixing was relatively unconstrained except for the assumption that  $d_1$  is smaller than  $d_0$  which seems justified. If the rate of  $D\bar{D}$  mixing is near the current experimental bounds, however, then there is another possible way to obtain  $\gamma$ . If one

measures  $\{d_0, d_1, \bar{d}_0, \bar{d}_1\}$  and knows all of the mixing parameters, then there are just four unknown parameters that need to be fitted for:  $\{\gamma, \delta, \zeta, \text{ and } b\}$ . We therefore have four equations in four unknowns and can solve for  $\gamma$ . To obtain  $d_1$  we can use the weight function:

$$w_1(\tau) = \tau - 1 \quad (81)$$

It is also possible to learn about  $\gamma$  using time integrated data. This has been previously considered in [23]. The corrections due to mixing in the approximation we are using are:

$$\begin{aligned} d &= d_0 + d_1 \\ \bar{d} &= \bar{d}_0 + \bar{d}_1 \end{aligned} \quad (82)$$

In the case that the  $D\bar{D}$  mixing parameters are already determined, if  $n$  modes are measured, there are  $3 + n$  unknowns:  $\zeta, \gamma, b$  and for each mode  $X_i, \delta_i$ . Each mode provides two pieces of information,  $d$  and  $\bar{d}$ , leading to a total of  $2n$  measurements. To solve for the unknowns at least 3 modes are thus required (six equations in six unknowns). If the mixing parameters are unconstrained, this adds four more unknowns:  $\{x, y, r_{qp}, \phi\}$  and in principle at least seven modes would be required.

On the other hand, using such time dependent information is probably not the best way to measure  $D\bar{D}$  oscillation parameters. Perhaps the best way to proceed is to consider  $d_1$  and  $\bar{d}_1$  to be corrections to the time integrated data. From eqn. (72) one can take the bound on  $x$  and  $y$  together with an estimate of  $b$  and bound these terms. As indicated, this gives about a 10% correction which, as discussed in [23] leads to about a  $15^\circ$  error in  $\gamma$ . This is similar to the errors typically obtained in the unmixed case for  $\hat{N}_B = 10^8$  and so to gain improvements in the determination  $\gamma$  with larger numbers of  $N_B$  in this scenario one would both have to improve the bounds on  $D\bar{D}$  mixing (or indeed discover it). Of course since measurements of  $D\bar{D}$  mixing can often be made at a  $B$  facility, it would be natural for such improvements to occur at the same time.

## References

- [1] L. L. Chau and W.-Y. Keung, Phys. Rev. Lett. **53**, 1802 (1984).
- [2] M. Gronau and D. Wyler, Phys. Lett. **B265** (1991); M. Gronau and D. London., Phys. Lett. **B253**, 483 (1991).
- [3] I. Dunietz, Phys. Lett. **B270**, 75 (1991).
- [4] I. Dunietz, Z. Phys. **C56**, 129 (1992).
- [5] I. Dunietz, “CP Violation with Additional B Decays”, published in B Decays, S. Stone ed. (World Scientific, Singapore, 1992).
- [6] D. Atwood, I. Dunietz and A. Soni, Phys. Rev. Lett. **78**, 3257 (1997).
- [7] T. E. Browder, K. Honscheid and D. Pedrini, Ann. Rev. Nucl. Part. Sci. **46**, 395 (1996); see also M. Neubert, V. Riekert, Q. P. Xu and B. Stech in *Heavy Flavors*, A. J. Buras and H. Linder (World Scientific, Singapore, 1992).
- [8] Particle Data Group, Z. Phys. **C3**, 1 (1998).
- [9] A. Ali and D. London, Eur. Phys. J. **C9**, 687 (1999);
- [10] N. Sinha and R. Sinha, Phys. Rev. Lett. **80**, 3706 (1998).
- [11] H. Yamamoto, Proceedings, Fourth International Workshop on Particle Physics Phenomenology, Kiohsung, Taiwan (1998) hep-ph/9812279.
- [12] A. Soffer, Phys. Rev. **D60**, 054032 (1999).
- [13] A. Soffer, hep-ex/9801018.
- [14] P. L. Frabetti *et al.*, Phys. Lett. **B331**, 217 (1994).
- [15] D. Atwood and A. Soni, Phys. Rev. **D45**, 2405 (1992); J. F. Gunion, B. Grzadkowski and X. He, Phys. Rev. Lett. **77**, 5172 (1996).
- [16] Z. Xing, Phys. Rev. **D55**, 196 (1997); T. Liu, *Tau Charm Factory Workshop*, Argonne IL (1995).
- [17] E. M. Aitala *et al* [E791 Collaboration], Phys. Rev. Lett. **83**, 32 (1999).

- [18] R. Godang *et al.* [CLEO Collaboration], hep-ex/0001060.
- [19] J. M. Link *et al.* [FOCUS Collaboration], hep-ex/0004034;
- [20] J. F. Donoghue, E. Golowich, B. R. Holstein and J. Trampetic, Phys. Rev. **D33**, 179 (1986)
- [21] M. Gronau, Phys. Rev. Lett. **83**, 4005 (1999).
- [22] H. N. Nelson, hep-ex/9908021.
- [23] J. P. Silva and A. Soffer, Phys. Rev. **D61**, 112001 (2000).

Table 1: Cabibbo allowed (CBA) and doubly Cabibbo suppressed (DCS) modes of  $D^0(\overline{D}^0)$ .  $BR$ 's for CBA modes are taken from PDB [8] while those for DCS are predicted, using the model given in the text, except for  $\overline{D}^0 \rightarrow K^+\pi^-$  wherein the measured value is shown.

Mode	$Br(D^0 \rightarrow \text{final state})$	$Br(\overline{D}^0 \rightarrow \text{final state})$
$K^+\pi^-$	$(2.9 \pm 1.4) \times 10^{-4}$	$3.83 \times 10^{-2}$
$K^+\rho^-$	$3.8 \times 10^{-4}$	$10.8 \times 10^{-2}$
$K^+a_1^-$	$7.0 \times 10^{-5}$	$7.3 \times 10^{-2}$
$K^{*+}\pi^-$	$8.3 \times 10^{-4}$	$5.0 \times 10^{-2}$

Table 2: The branching ratios for the combined decay  $B^- \rightarrow K^{*-} D^0$  followed by the decay of  $D^0$  to the modes given below using the parameters considered in Section 6 with  $\gamma = 60^\circ$  and the given strong phases  $\xi_i$ .  $d_i$  and  $\bar{d}$  are given in units of  $10^{-8}$  and  $\alpha'$  is the partial rate asymmetry.

Mode	$d_i$	$\bar{d}_i$	$\frac{1}{2}(d_i + \bar{d}_i)$	$\alpha'$	$\xi_i$
$K^+ \pi^-$	91	75	83	0.096	10
$K_s \pi^0$	842	740	791	0.064	20
$K^+ \rho^-$	289	159	224	0.288	30
$K^+ a_1^-$	203	90	146	0.383	40
$K_s \rho^0$	333	391	362	0.081	200
$K^{*+} \pi^-$	97	34	65	0.477	50

Table 3: The parameters of the model for  $D^0 \rightarrow K^- \pi^+ \pi^0$  decay obtained in [14].

channel	decay fraction (%)	$\delta_r - \delta_\rho$ (deg.)
non-resonant	$10.1 \pm 3.3 \pm 3.0 \pm 2.7$	$-122 \pm 10 \pm 21 \pm 2$
$K^{*0}$	$16.5 \pm 3.1 \pm 1.1 \pm 1.1$	$-2 \pm 12 \pm 23 \pm 2$
$K^{*+}$	$14.8 \pm 2.8 \pm 4.9 \pm 0.3$	$162 \pm 10 \pm 7 \pm 4$
$\rho^-$	$76.5 \pm 4.1 \pm 2.2 \pm 4.9$	0

## Figure Captions

**Figure 1:** Each of the solid lines shows the locus of points in  $\gamma$  versus  $u_i$  of allowed solutions given  $z_i = 1.5$  for  $y_i = 0$  (outer curve), 1 (intermediate curve) and 2 (inner curve). The boxes indicate the inequalities Eqns. (30,33).

**Figure 2:** The solid line shows the allowed points on the  $\gamma - b(K^*)$  plot given a measurement of  $B^- \rightarrow K^* D^0$  followed by  $D^0 \rightarrow K^+ \pi^-$  (and charge conjugate) using the estimated values of Section 5 eqns. (43,45) assuming  $\gamma = 90^\circ$ . The dashed line shows the results which would follow in the same case given a measurement of  $D^0 \rightarrow K_s \pi^0$  in the final state.

**Figure 3:** (a) The likelihood distribution is shown as a function of  $\gamma$  and  $b(K^*)$  assuming that  $\tilde{N}_B^{3\sigma} = 10^8$  with the branching ratios considered in Table 2 and assuming only the  $K^+ \pi^-$  and  $K_s \pi^0$  modes are measured. The outer edge of the shaded regions correspond to 90% confidence while the inner edge corresponds to 68% confidence. The solid lines show the locus of points which give exactly the  $K^+ \pi^-$  results while the short dashed curve shows the points which give the  $K_s \pi^0$  results.

(b) The likelihood distribution as in Fig. 3a is shown assuming all of the modes in Table 2 are used. The solution for the  $K^+ \pi^-$  data is shown with the solid curve; that for the  $K_s \pi^0$  data is shown with the short dashed curve; the one for the  $K^+ \rho^-$  data is shown with the long dashed curve; the one for the  $K^+ a_1^-$  data is shown with the dash-dot curve; the one for the  $K_s \rho^0$  data is shown with the dash-dot-dot curve and the solution for the  $K^{*+} \pi^-$  data is shown with the dash-dash-dot curve.

**Figure 4:** The ratio between the the likelihood distribution and the maximum likelihood is shown as a function of  $\gamma$  with the parameters as in Fig. 3b except  $\gamma$  is taken to be  $15^\circ$  (dashed curve);  $30^\circ$  (solid curve);  $60^\circ$  (dotted curve);  $90^\circ$  (dash-dot curve).

**Figure 5:** (a) Dalitz plots for the decay products of the  $D^0$  in the decay chain  $B^- \rightarrow K^{*-} D^0$  followed by  $D^0 \rightarrow K^+ \pi^- \pi^0$  (upper plot) and the charge conjugate process (lower plot). We use the model described in

section 6 where we take  $\gamma = 90^\circ$  and  $\xi = 90^\circ$ . The plots represent the results given  $N_B = 10^{10}$ .

(b) Dalitz plot for the same system as in Fig. 5(a) with  $\xi = 0^\circ$ .

**Figure 6:** (a) A plot of the partial rate asymmetry for the system in Fig. 5 as a function of  $\gamma$ .

(b) The  $N_B$  required for a  $3 - \sigma$  signal as a function of  $\xi$  using only the PRA (solid line) and using the optimal observable (dashed line).

**Figure 7:** (a) The locus of points on a dalitz plot where  $Q_{min} = Q$  for  $\gamma = 60^\circ$  and  $\zeta = 0^\circ$  (solid line);  $\zeta = 30^\circ$  (dashed line);  $\zeta = 60^\circ$  (dotted line) and  $\zeta = 90^\circ$  (dot-dashed line).

(b) A plot of  $f(rQ)$  as a function of  $\gamma$  for  $\zeta = 0^\circ$  (solid curves); for  $\zeta = 30^\circ$  (dashed curves); for  $\zeta = 60^\circ$  (dotted curves) and for  $\zeta = 90^\circ$  (dash-dot curves). In each case the lower curve corresponds to  $r = 0.9$  and the upper curve to  $r = 0.7$ .

(c) A plot of  $f^2(q)$  is shown as a function of  $q$  for  $Q = 3/4$  (solid line);  $Q = 1/2$  (dashed line) and  $Q = 1/4$  (dotted line) where  $\zeta = 90^\circ$ .

**Figure 8:** A plot of  $g_{min}^2(b)$  (solid line) and  $g_{max}^2(b)$  (dashed line) line is shown as a function of  $b/b(k)$ . Here we have taken  $Q = 3/4$  and  $\zeta = \pi/2$ .



Figure 1

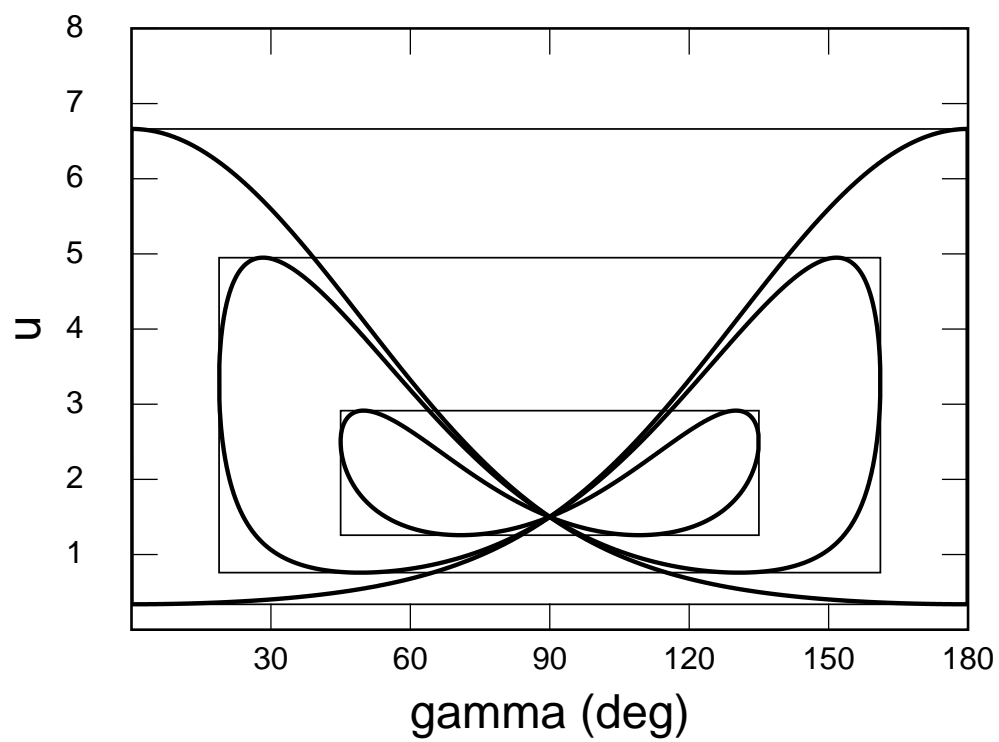


Figure 2

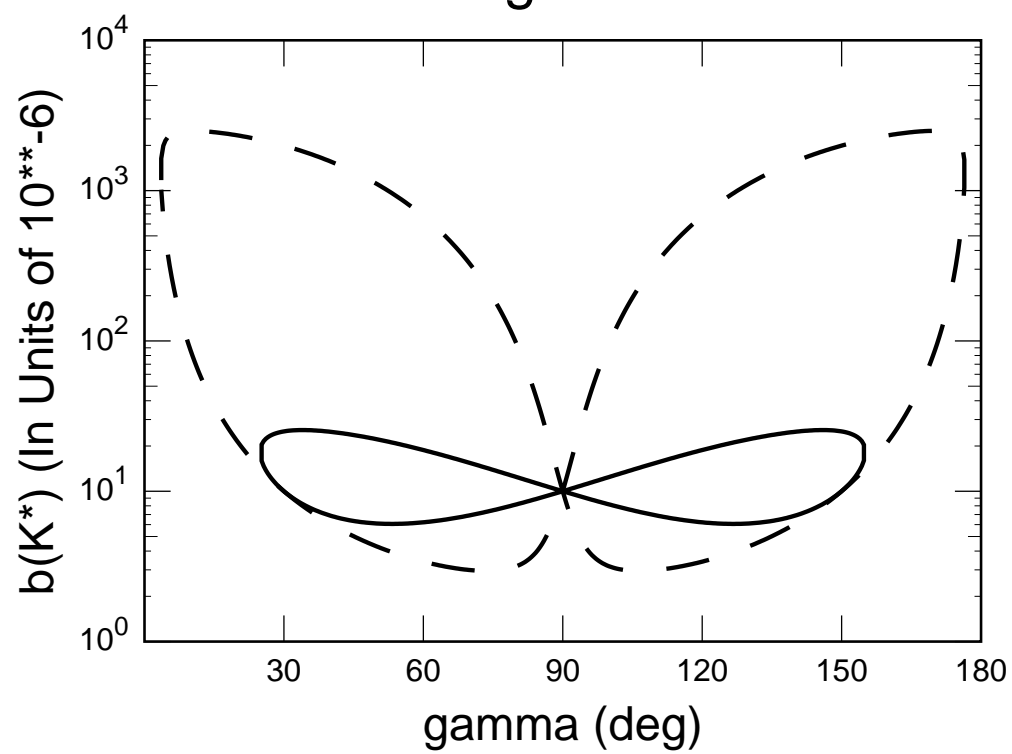


Figure 3a

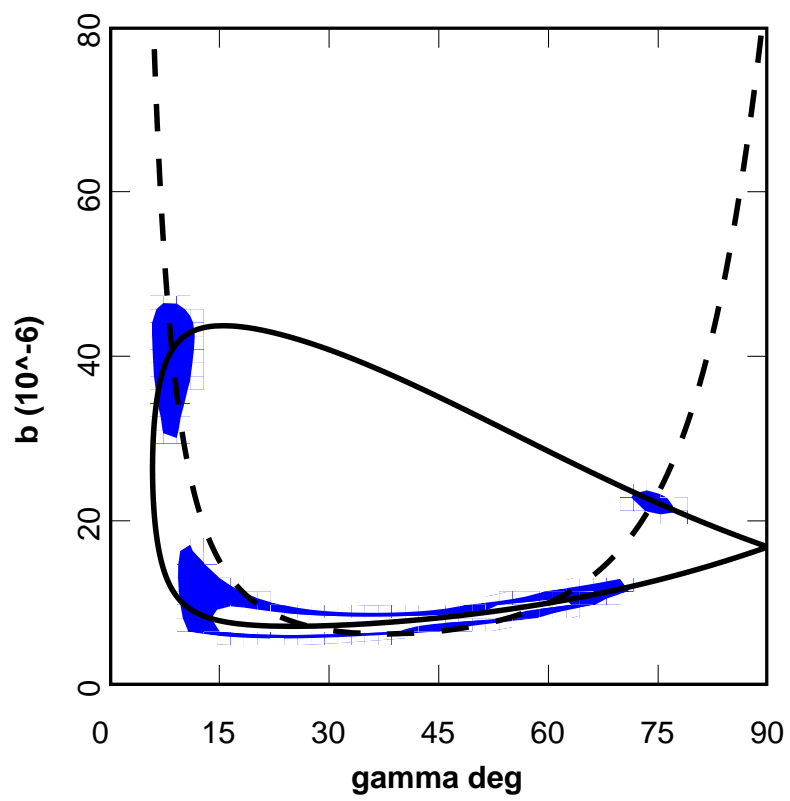


Figure 3b

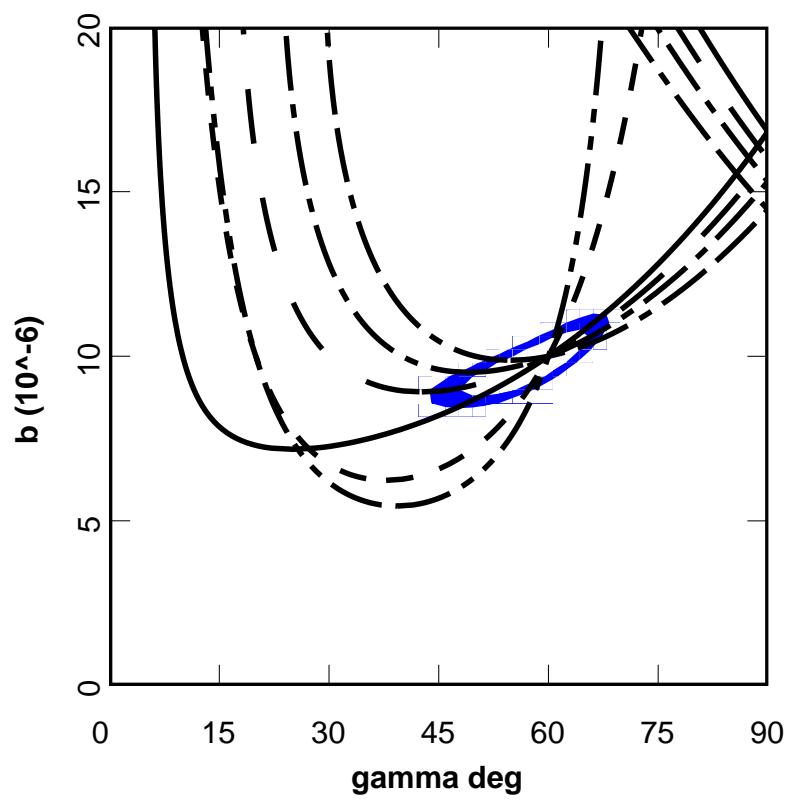
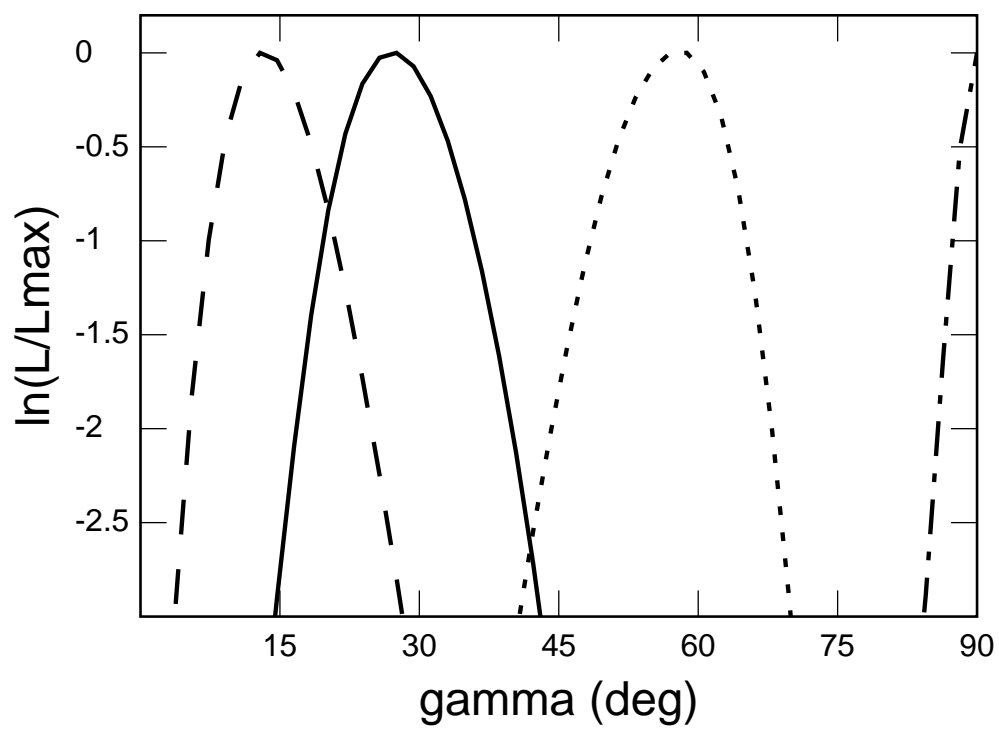
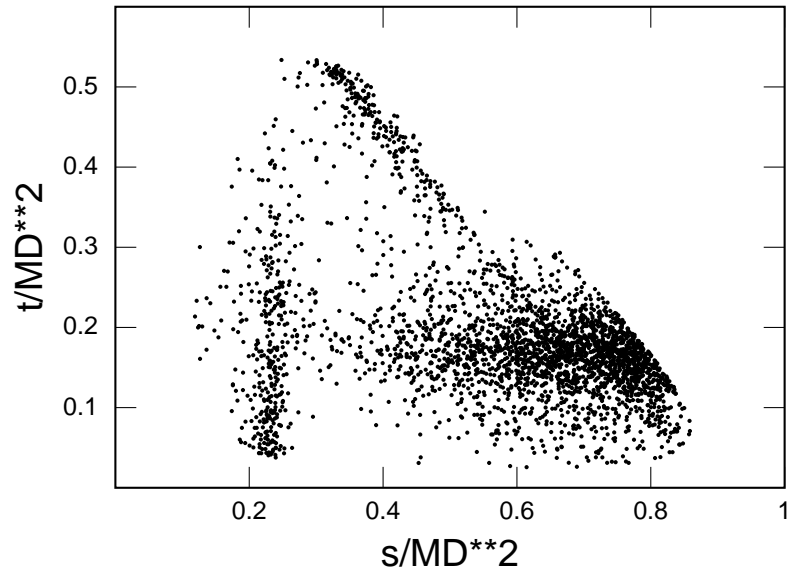


Figure 4



## Figure 5a

B-  $\gamma = 90.0$   $\zeta = 70.0$



B+  $\gamma = 90.0$   $\zeta = 70.0$

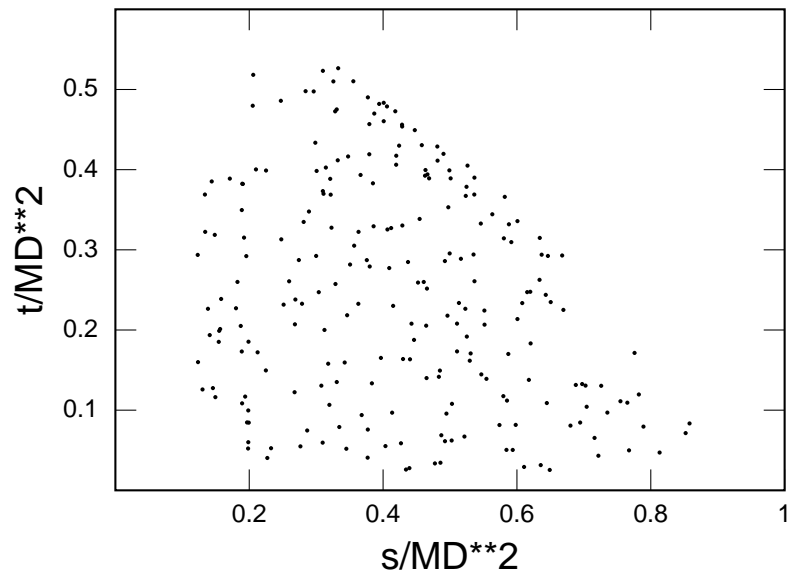
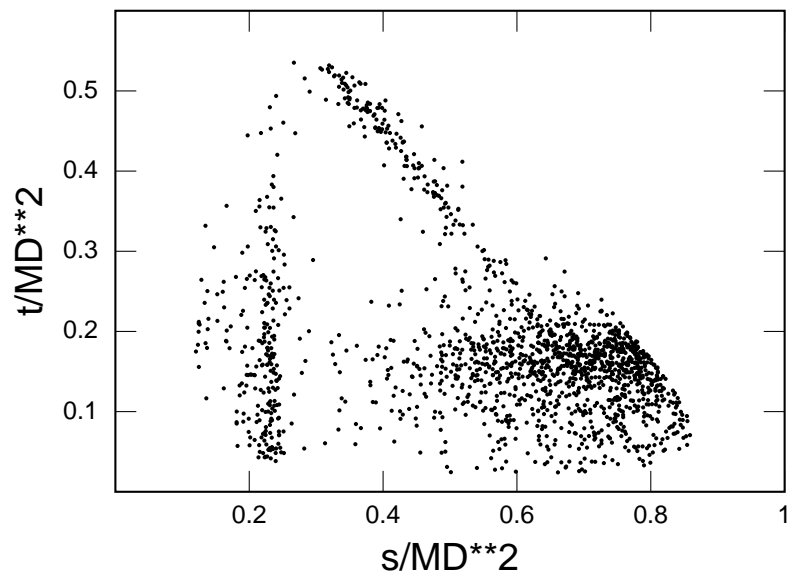


## Figure 5b

B- gamma= 90.0 zeta= 160.0



B+ gamma= 90.0 zeta= 160.0

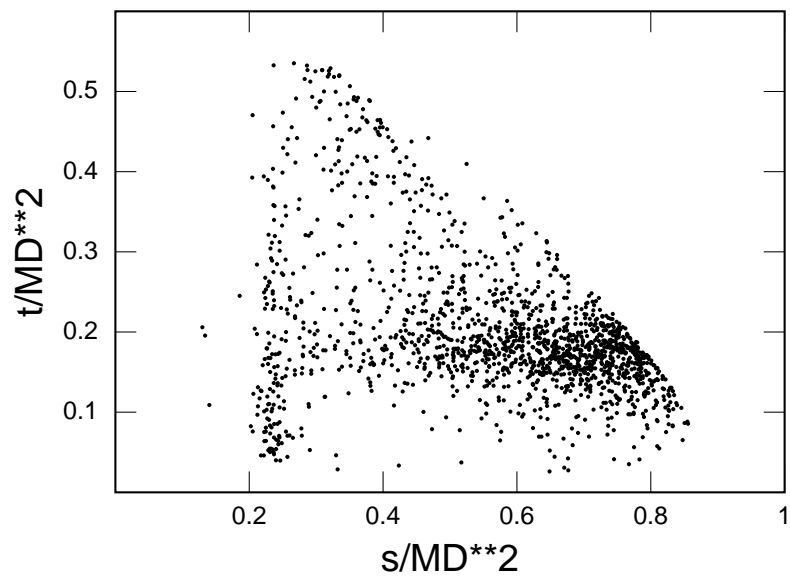


Figure 6a

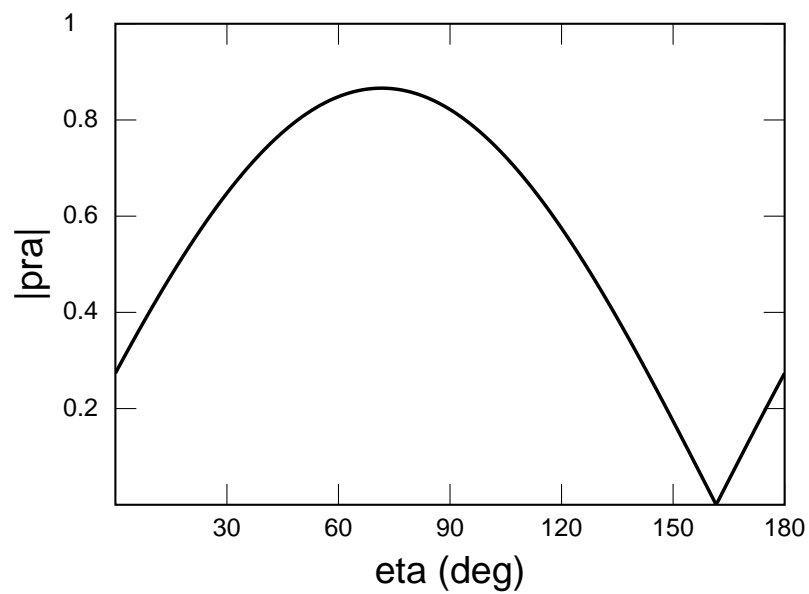


Figure 6b

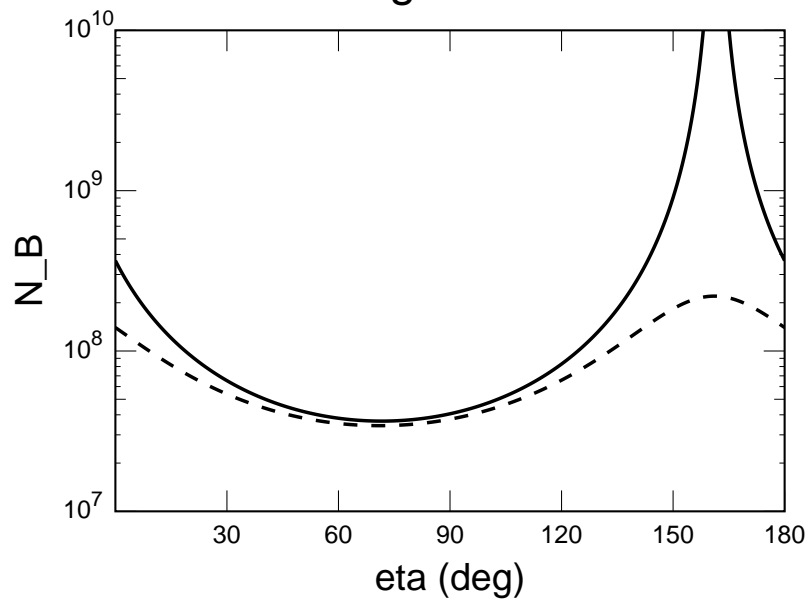




Figure 7a

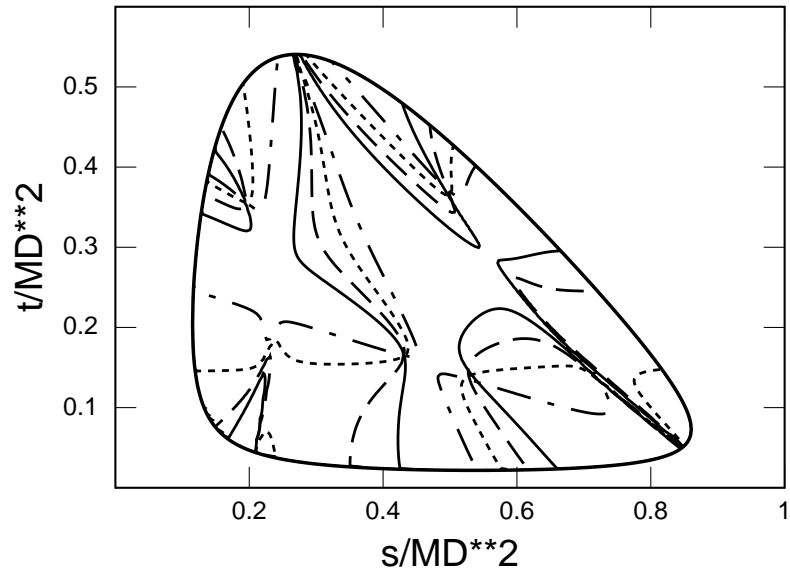


Figure 7b

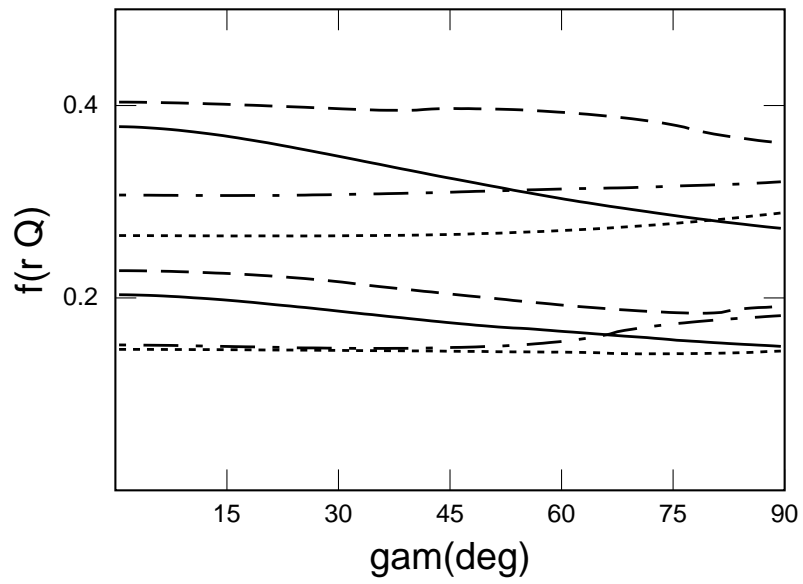


Figure 7c

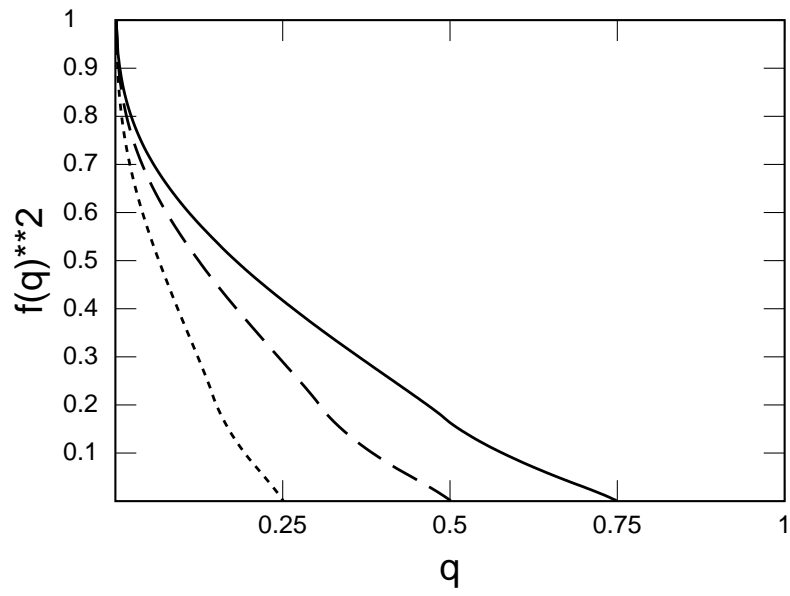


Figure 8

